Journal of Analytical and Applied Pyrolysis 169 (2023) 105856

Contents lists available at ScienceDirect

Journal of Analytical and Applied Pyrolysis

journal homepage: www.elsevier.com/locate/jaap

Recent advances on activated carbon-based materials for nitrate adsorption: A review

M.J. Ahmed [a,*], B.H. Hameed [b], M.A. Khan [c]

[a] Department of Chemical Engineering, College of Engineering, University of Baghdad, 10071, Baghdad, Iraq
[b] Department of Chemical Engineering, College of Engineering, Qatar University, P.O. Box 2713, Doha, Qatar
[c] Chemistry Department, College of Science, King Saud University, Riyadh 11451, Saudi Arabia

ARTICLE INFO

Keywords:
Activated carbon
Adsorption
Nitrate
Performance
Reusability

ABSTRACT

Nitrate contaminant has a real impact on aquatic environmental systems and public health due to its increasing discharge from agricultural and industrial activities. In particular, high nitrate amount in water can cause eutrophication and different diseases, such as blue baby syndrome. Thus, the removal of nitrate from aquatic ecosystems is essential for preventing such issues. For this purpose, adsorption has been adopted in many studies as a simple, efficient, and eco-friendly technique. Moreover, activated carbon (AC)-based adsorbents exhibit high removal performance towards nitrate owing to their unique pore characteristics and functional groups enriched structures. This article represents a comprehensive review on the production, characterization, and application of AC-based adsorbents for nitrate removal from water. The most common forms of AC-based adsorbents such as raw, modified, and composite are considered. The influences of preparation and adsorption variables on nitrate removal performance of such adsorbents are explained. Furthermore, the nitrate adsorption behavior under batch, fixed bed, and competitive operations along with the mechanism and adsorbents reusability is also discussed. Finally, the conclusions and future trends for the studied adsorption systems are given.

1. Introduction

Nitrate is an inorganic anion that contains one nitrogen atom and three oxygen atoms, the chemical symbol for nitrate is NO_3^- [1]. This anion has been classified as one of the most widespread contaminants owing to its high water solubility [2]. The existence of large amounts of NO_3^- in water due to overuse of fertilizers and discharge of harmful wastes from industrial and municipal activates, has become a severe environmental threat to the world. It leads to eutrophication which can result in excessive aquatic plant growth, algae growth, harm to fish and other organisms, and disruption of the natural balance of species in the water [3]. Moreover, high NO_3^- concentration in drinking water can lead to serious health issues in terms of infant methemoglobinemia or "blue baby" syndrome and stomach cancer [4]. Therefore, the World Health Organization (WHO) identifies a maximum NO_3^- amount of 50 mg/L in drinking water [5].

Several methods have been adopted for the elimination of nitrate from water including ion exchange [6], reverse osmosis [7], electrodialysis [8], biological denitrification [9], and chemical reduction [10]. However, these methods have several limitations despite their high performance. For instance, ion exchange requires post-treatment and waste brine disposal, reverse osmosis has a very high operating cost, catalytic reduction produces ammonia as undesirable byproduct, and biological denitrification creates large amounts of biomass and microbes that need additional treatments. Furthermore, the latter method is unfavorable for treating of inorganic pollutants due to the requirement of extra organic substrates to act as electron donors [11].

On the other hand, adsorption is often regarded as the most appealing owing to its suitability, operation flexibility, design simplicity, and cost-affectivity if cheap and simply regenerated adsorbents are utilized [3]. Nitrate removal by adsorption mainly depends on the contact between nitrate and adsorbent followed by the movement of nitrate ions from solution bulk towards adsorbent surface. For this purpose, the selection of appropriate adsorbents and best adsorption variables play a significant role in efficient removal of nitrate [12]. Several adsorbents including resin, silica, biochar, graphene, clay or organoclay, carbon nanotubes, alumina, zeolite, soils, Mg–Al layered double hydroxide, chitosan, agricultural biomass, and hydroxyapatite have been used to adsorb nitrate [13–25]. However, some of these materials are not highly effective and exhibit small to medium nitrate

* Corresponding author.
E-mail address: muthanna.ja@gmail.com (M.J. Ahmed).

https://doi.org/10.1016/j.jaap.2022.105856
Received 14 September 2022; Received in revised form 23 December 2022; Accepted 30 December 2022
Available online 30 December 2022

uptakes due to their low porosity and functionality and the others are considered high cost adsorbents. Using activated carbon (AC)-based materials among these adsorbents has higher economic and environmental advantages [26]. These adsorbents can be obtained from a variety of agricultural and industrial wastes. AC has the advantage of high removal efficiency due to its large surface area and favorable functionality. Moreover, the use of modified and composite forms of AC is able to enhance its surface and textural characteristics and eventually, can improve the efficiency of adsorption [3,12]. To this end, we have examined carbon-based adsorbents in the following parts.

Many reviews have considered the adsorption of nitrate onto biochar and its modifications [27,28], chitosan and chitosan derivatives [29,30], clays in the raw and modified forms [31], emerging adsorbents (zeolite, chitosan, agricultural wastes, etc.) [11], solid waste bio-adsorbents [1], and agricultural wastes [32]. AC has been indicated in some reviews [11,12,26,33–35]. However, such reviews did not consider the production, characteristics, adsorption utilization, and reuse of AC-based adsorbents in detail. Thus, this paper is an up to date review of literature on the utilization of AC-based adsorbents for nitrate removal involving the production and modification techniques, properties, performance, isotherms, kinetics, thermodynamics, and mechanisms. Competitive and fixed bed adsorption behaviors of the studied system along with regeneration and reuse of adsorbents were also included.

2. Methodology

This article reviewed the data of 84 studies published between 2010 and 2022 on the adsorption behavior of nitrate on AC-based adsorbents. Six studies found in the literature from 2003 to 2009 were also included as they presented significant data. The major sources of these studies were the Scopus database and Google Scholar, and the main keywords applied for collecting the data were “AC-based adsorbents”, “adsorption”, and “nitrate”. The obtained data were summarized in Tables 1–5 and discussed in three sections. The data for preparation studies including the characteristics of AC-based adsorbents obtained by different methods under various conditions were presented in Table 1 and discussed in Section 3. The data for isotherms, kinetics, and thermodynamics of nitrate adsorption on AC-based adsorbents were given in Tables 2–4 and discussed in Sections 5–7. The data for desorption and reuse studies of AC derived adsorbents saturated with nitrate were presented in Table 5 and discussed in Section 11. Finally, the findings and recommendations for further research are given based on the analysis of the obtained data.

3. Activated carbon-based adsorbents

Activated carbons in the raw, modified, and composite forms have been widely used for the adsorption of inorganic anions such as nitrate. Table 1 summarizes the characteristics of AC-based adsorbents derived from a variety of precursors using different activating agents under specific conditions. According to this table, most of the studies include the chemical activation process as compared to the physical and physicochemical activations. This section discusses the production and modification techniques along with characteristics of AC-based adsorbents.

3.1. Raw activated carbon

Activated carbon is a carbon enriched solid with a developed structure that includes high porosity, diverse pores, and abundant active sites [36]. Thus, AC is an efficient adsorbent for wastewaters treatment. However, AC properties are varying with its precursors and production technique. The most adopted precursors for commercial ACs are highly cost and non-renewable like coal and petroleum precursors [37]. ACs are recently produced from agricultural and industrial wastes for a cost-effective adsorption system [38,39].

Physical and chemical activations along with physiochemical one are the basic methods being used for the preparation of ACs [40,41]. Physical process involves the pyrolysis of precursors in the absence of oxygen and activation of the obtained char at elevated heating using CO_2 or steam as oxidizing agent. In the chemical process, pyrolysis and activation may be carried out in a one-step using chemicals like $ZnCl_2$, H_3PO_4, NaOH, and KOH at moderate heating [42]. Chemical process exhibits ACs with high porosity, more quantity, and needs lower heating than physical process. However, this process is accompanied with corrosion issue, washing step requirement, and poor separation of excess activators, which may pollute water during adsorption application [43]. Physiochemical activation involves the mixing of precursors with a chemical agent, followed by an activation step with a physical agent. The benefits of this type of activations are its controllable textural features and surface development. However, the complexity and high energy requirements of physiochemical activation limit its practical applicability [44].

Raw ACs have been widely adopted as efficient adsorbents for nitrate [45–57]. According to the collected data, chemical activation is the most frequently used process for the production of AC adsorbent for removal of nitrate. Moreover, the commonly used activating agents are $ZnCl_2$, H_3PO_4, H_2SO_4, KOH, K_2CO_3, NaOH, Na_2CO_3, HCl, and $CaCl_2$. Among these agents, $ZnCl_2$ was the most applied agents for production of AC. In this context, AC with a large surface area of 1826.0 m^2/g was obtained from sugar beet bagasse by $ZnCl_2$ activation. In brief, the bagasse precursor was added to a solution of $ZnCl_2$ in 300 mL distilled water at 3:1 (g/g) impregnation ratio and agitated at 80 °C for 6 h. The sample was then put in a stainless steel boat and pyrolyzed in an electrical furnace at 700 °C for 90 min under the heating extent of 5 °C/min and N_2 flow of 100 mL/min. The obtained AC was sequentially rinsed with 0.5 M HCl solution and warm distilled water till the pH of filtrate attained 6 [51]. The favorable activation by $ZnCl_2$ relative to other agents such as HCl, H_2SO_4, KOH, and H_3PO_4 was also reported for production of AC from finnish wood chips biochar precursor. The specific surface area of AC was about 20 times that of its precursor. Moreover, the adsorption performance of AC was about 3 times that of its precursor [55]. However, the largest surface area (2802.0 m^2/g) was reported for AC that obtained by NaOH activation of rice husk. NaOH agent exhibited AC with more developed microporous structure and low ash content. This could be related to the fact that NaOH was reacted with SiO_2 which resulted in opening of blocked pores [49]. For physical activation, steam was more applied to produce AC relative to CO_2. In this context, AC with a surface area of 1073.98 m^2/g was derived from bamboo char precursor by steam activation. Precursor particle with a specific size was placed in a quartz tube inside a muffle furnace, and the temperature was elevated to 850 °C at a heating extent of 10 °C/min. Then, steam was supplied at a flow rate of 6.5 g/min, and the activation was performed for 1 h, followed by oven drying of AC product [58]. The maximum reported surface area for steam and CO_2 ACs were 1144.0 and 590.0 m^2/g from coconut shells [59] and Finnish wood chips [60] precursors, respectively. Physicochemical activation was also reported for production of AC. In this regard, oil palm shell char was impregnated with KOH or H_3PO_4 solution, agitated for 24 h at 60 °C, and then dehydrated at 120 °C for 24 h. The impregnated samples were activated at an average temperature of 700 °C for 3 h under steam flow rate of 0.1 mL/min. After that, both samples were thoroughly rinsed with distilled water to reach pH 6–7. KOH-steam and H_3PO_4-steam ACs exhibited surface areas of 838.03 and 564.03 m^2/g, respectively.

3.2. Modified activated carbon

Adsorption performance of raw activated carbons towards nitrate ions can be further improved by chemical modification. The improvement in performance of AC mainly depends on enhancement of its functionality by introducing additional and specific functional groups [3]. In some cases the pore properties of raw AC adsorbent can also be

Table 1
Pore properties, elemental content, and other characteristics of different AC-based adsorbents used for nitrate removal.

Precursor/activator	Adsorbent	Preparation conditions	Pore properties			Elemental content (%) & other properties	Ref.
			S_{BET} m^2/g	V_t cm^3/g	dp nm		
Finnish wood chips/CO_2	Raw AC	800 °C, 3 h, 10 °C/min, 0.09 L/min CO_2	590.0	0.335	3.44	C 52.1, H 0.4, N < 0.5, O < 8, S< 2	[45]
Coconut shells/ Steam	Raw AC		786.0	0.435	2.21	C 91.9, H 0.5, N < 0.5, O 2.6, S< 2	[45]
Commercial	Raw AC		374.4	0.530	7.22	C 87.48, N 0.0, O 11.40, Si 0.51, P 0.61	[46]
Orange peel/H_3PO_4	Raw AC	450 °C, 0.5 h, 2:1 H_3PO_4/ precursor	1090.0	1.056		pH_{PZC} 5.5	[47]
Almond shells/steam	Raw AC	850 °C, 1 h, 0.1 g/min steam	641.0	0.351		pH_{PZC} 10.6	[47]
Oil palm shells/H_3PO_4-steam	Raw AC	600–800 °C, 3 h, 0.1 mL/min steam	564.03	0.230	2–4		[48]
Oil palm shells/KOH-steam	Raw AC	600–800 °C, 3 h, 0.1 mL/min steam	838.03	0.390	2–4		[48]
Rice husk/NaOH	Raw AC	800 °C, 3 h, 3:1 NaOH/ precursor	2802.0	1.690	1.210	Ash 3.52 %	[49]
Coir pith/$ZnCl_2$	Raw AC	700 °C, 2:1 $ZnCl_2$/precursor	910.0	0.363	1.600	Fixed C 81 %, volatiles 19 %, ash 3.2 %, pH_{PZC} 3.2	[50]
Sugar beet bagasse/ $ZnCl_2$	Raw AC	700 °C, 1.5 h, 5 °C/min, 100 mL/min N_2, 3:1 $ZnCl_2$/precursor	1826.0	0.966	2.220		[51]
P. juliflora branches/ H_2SO_4	Raw AC	500 °C, h, 1:1 H_2SO_4/precursor	358.47	0.189	1.555	C 74.09, O 17.60, N 7.65, P 0.67	[52]
Rice straw/Na_2CO_3	Raw AC	650 °C, 1 h, Na_2CO_3	122.9	0.099		C 8.97, H 0.46, O 6.57, N, ash 72.8 %	[53]
Shrimp shell/$ZnCl_2$	Raw AC	400 °C, 2 h, 2:1 $ZnCl_2$/ precursor, 5 °C/min	1536.3	0.830	2.42		[54]
Finnish wood chips/ $ZnCl_2$	Raw AC	500 °C, 1 h, 5 M $ZnCl_2$, 10 w/w L/S ratio	285.0	0.260	3.940	C 61.8, H 0.75, N 1.6, S < 2	[55]
G. globra residues/$ZnCl_2$	Raw AC	850 °C, 1 h, 2:1 $ZnCl_2$/ precursor, 200 mL/min N_2, 10 °C/min	959.22	0.543	2.223	C 83.24, O 11.92, Cl 3.44, Zn 1.40	[56]
P. aculeate trunks /K_2CO_3	Raw AC	800 °C, 2 h, 1:1 K_2CO_3/ precursor	777.0	0.350	1.810	C 80.6, H 1.6, O 17.4, N 0.4, pH 7.2	[57]
P. aculeate trunks /NH_4Cl	Raw AC	450 °C, 0.5 h, 0.1:1 NH_4Cl/ precursor	58.0	0.030	1.910	C 65.4, H 3.1, O 25.2, N 6.3, pH 4.1	[57]
Commercial	HNO_3 modified AC		1090.0	0.666		C 95.18, H 0.16, O 3.50, N 1.16	[62]
Commercial	Raw AC		1146.0	0.612		C 90.84, H 0.09, O 8.51, N 0.56	[62]
Coconut shell/ commercial	NaOH modified AC		901.0	0.490			[63]
Coconut shell/ commercial	NaOH-CTAB modified AC		722.0	0.420			[63]
Commercial	CTAC modified AC		926.8	0.589	0.599		[64]
Commercial	Raw AC		1359.6	0.809	0.549		[64]
Corn straw/ H_3PO_4	$FeCl_3$ modified AC		217.87	0.429	3.470	C 53.24, H 1.32, N 0.52, O 14.95	[65]
Corn straw/ H_3PO_4	Raw AC	600 °C, 1.5 h, H_3PO_4 85 %	563.93	1.087	2.260	C 75.81, H 1.01, N 0.75, O 10.89	[65]
Almond shells/H_3PO_4	Magnetic AC		150.48			C 44.42, O 32.77, Na 0.7, S 0.64, Fe 19.66	[66]
Almond shells/H_3PO_4	Raw AC	700 °C, 1 h, 1:1 H_3PO_4/ precursor	54.254				[66]
Grape wood/H_2SO_4	Iron modified AC		1050.0	0.284	2.50	C 49.8, O 7.48, N 12.2	[67]
Grape wood/H_2SO_4	Raw AC	550 °C, 2 h, 2 M H_2SO_4	1169.0	0.338	3.30	C 98.43, O 1.0, N 0.57	[67]
Pine cones/H_3PO_4	Urea modified AC	100 % urea for 24 h at 110 °C, then at 350 °C, 3 h, 50 °C/min	449.0	0.20	2.200	C 67.0, H 2.3, N 13.0, O 17.6, pH_{PZC} 6.0	[68]
Pine cones/H_3PO_4	Raw AC	450 °C, 0.5 h, 2:1 H_3PO_4/precursor., 3 °C/min	1082.0	0.700	2.500	C 88.2, H 3.4, N 0.4, O 8.0, pH_{PZC} 5.1	[68]
Rice husk/K_2CO_3	Urea modified AC	950 °C, 1 h, 4:1 K_2CO_3/precursor, Ar flow	1330.0	1.337	4.020	C 92.3, O 5.16, Si 1.45, K 1.66	[69]
P. aculeate sawdust/ H_3PO_4	Urea modified AC	2:1 urea/AC, 110 °C, 24 h, 350 °C, 3 h, 50 K/min	308.0	0.170	2.20	C 67.5, H 3.2, O 16.2, N 13.1, pH_{PZC} 5.7	[70]
P. aculeate sawdust/ H_3PO_4	Raw AC	450 °C, 0.5 h, 2:1 H_3PO_4/precursor	968.0	0.700	2.900	C 77.0, H 2.5, O 20.2, N 0.3, pH_{PZC} 5.1	[70]
P. aculeate sawdust/KOH	Urea modified AC	2:1 urea/AC, 110 °C, 24 h, 350 °C, 3 h, 50 K/min	191.0	0.090	2.00	C 73.7, H 1.6, O 9.9, N 14.8, ash 11 %, pH_{PZC} 6.9	[70]
P. aculeate sawdust/KOH	Raw AC	800 °C, 2 h, 150 mL/min N_2 flow, 1:1 KOH/ precursor	768.0	0.370	1.900	C 74.7, H 0.5, O 24.3, N 0.5, pH_{PZC} 6.8,	[70]
C. manni naudin shells/ $ZnCl_2$	Amine modified AC		113.43	0.080	2.480	C 61.68, H 0.97, O 28.39, N 8.96, pH_{PZC} 8.6	[71]
C. manni naudin shells/ $ZnCl_2$	Raw AC	698 °C, 0.5 h, 10 M $ZnCl_2$	1008.99	0.590	2.020	C 71.55, H 0.39, O 27.07, N 0.99, pH_{PZC} 7.0	[71]
Sucrose/H_2SO_4	Amino modified AC		599.82	0.467	2.440	C 60.91, O 37.88, N 1.22	[72]
Sucrose/H_2SO_4	Raw AC	900 °C, 6 h	985.7	0.559	3.320	C 75.37, O 16.80, Na 7.83	[72]
Coconut/commercial	$ZnCl_2$ modified AC	500 °C, 1 h, 2:1 $ZnCl_2$/ precursor	567.52	0.253	0.492	C 37.61, O 0.9, Al 7.38, Mg 0.49, Ca 53.61	[73]
Coconut/commercial	Raw AC		876.75	0.404	0.518	C 74.75, O 6.14, Al 3.29, Mg 15.21, Ca 0.61	[73]
Lignite/commercial	$ZnCl_2$ modified AC		1261.4	0.973	3.560	pH_{PZC} 5.9	[74]
Coconut shell/steam	$ZnCl_2$ modified AC	500 °C, 1 h, 2:1 $ZnCl_2$/ precursor	893.0	0.447		C 66.39, O 14.26, Cl 7.26, Zn 12.09	[59]
Coconut shell/steam	Raw AC		1144.0	0.416		C 89.65, O 5.64, Cl 0.69, Zn 4.02	[59]
Strip moso bamboo/ H_3PO_4	quaternary nitrogen (acetonitrile vapor) modified AC		995.0	1.090	4.40	C 78.4, H 0.4, O 17.1, N 4.1	[75]
Strip moso bamboo/ H_3PO_4	Raw AC	500 °C, 1 h, 15 C/min, N_2 flow, 6:1 H_3PO_4/ precursor	1024.0	1.750	6.80	C 72.3, H 1.4, O 26.3, N 0.0	[75]
Polyacrylonitrite fiber/ $ZnCl_2$	Quaternary nitrogen modified AC	700 °C, 0.5 h, 4:1 $ZnCl_2$/precursor	1140.0	0.560	2.00	C 82, H 0.5, O 12, N 4.7	[76]

(*continued on next page*)

Table 1 (*continued*)

Precursor/activator	Adsorbent	Preparation conditions	Pore properties			Elemental content (%) & other properties	Ref.
			S_{BET} m^2/g	V_t cm^3/g	dp nm		
Rice straw/steam	$KMNO_4$ modified AC		122.90	0.099		C 10.97, H 0.56, O 7.57, N, ash 65.8 %	[77]
Rice straw/steam	Raw AC	650 °C, 1 h, 5 mL/min steam 5 °C/min	76.20	0.064		C 31.0, H 1.21, O 1.42, N, ash 44.0 %	[77]
Almond shell/ commercial	Zn modified AC		9.490 %	0.349	45.562	Zn 1.4, moisture 6.26 %, density 0.3 g/cm^3, pH 5.39	[78]
Almond shell/ commercial	$ZnSO_4$ modified AC		9.389 %	0.339	45.326	Zn 1.8, moisture 6.73 %, density 0.29 g/cm^3, pH 5.9	[78]
Almond shell/ commercial	Raw AC		12.253 %	0.247	41.269	Zn 0, moisture 3.3 %, density 0.29 g/ cm^3, pH 6.71	[78]
Petroleum pitch/ commercial	$(NH_4)_2S_2O_8$ modified AC	50 L/kg at 25 °C for 7 d, then 950 °C for 5 min under NH_3gas	770.0	0.350	1.80	C 84.0, H 0.61, O 9.0, N 6.42, pH_{PZC} 4	[79]
Petroleum pitch/ commercial	Raw AC		1380.0	0.610	1.80	C 94.0, H 0.66, O 5.0, N 0.35, pH_{PZC} 7.1	[79]
Vetiver grass/KOH	ZR/CTAB modified AC		222.95	0.191	3.423	C 91.02, O 4.11, Br 3.92, Zr 0.94	[80]
Vetiver grass/KOH	Raw AC	850 °C, 30 min, 1:1 KOH/ precursor	1379.63	0.711	2.060	C 95.68, O 4.16, Br 0.09, Zr 0.07	[80]
Bamboo/steam	ZR/CTAB modified AC	ZR/CTAB & AC mixing at 25 °C for 24 h, then drying at 70 °C for 24 h	105.72	0.141	5.345		[58]
Bamboo/steam	Raw AC	850 °C, 1 h, 6.5 g/min steam, 10 °C/min	1073.98	0.608	2.266		[58]
Commercial	Fe^{2+}, H_2O_2 modified AC		895.1	0.472	2.10	C 81.16, O 12.80, Fe 2.34	[81]
Commercial	Raw AC		973.6	0.483	1.90	C 83.65, O 11.58, Fe 1.31	[81]
Banana bract/H_2SO_4	Amine/Fe_3O_4 modified AC	600 °C, 12 h, H_2SO_4	135.45	1.234	7.514	C, N, O, Cl, Fe	[82]
Orange peel/H_2SO_4	Zn-Fe LDHs/AC composite	600 °C, 12 h, 1 M H_2SO_4	157.90	0.231	7.412	C, N, O, Zn, Fe, pH_{PZC} 6.1	[95]
Apple branch/CO_2	Mg/Al-LDHs AC composite		257.64	0.161	6.250	C 43.71, H 1.97, O 14.6, N 0.65, Mg 15.76, Al 6.24	[60]
Apple branch/CO_2	Raw AC	500 °C, 2 h, CO_2	526.34	0.437	3.29	C 80.96, H 1.81, O 10.68, N 1.42, Mg 0.87, Al 0.94	[60]
Sewage sludge/$ZnCl_2$	Magnetic Mg-Fe/ LDHs AC composite		169.0	0.210	1.820	C 12.6, O 34.8, Mg 13.3, Fe 55.3, Si 1.5	[96]
Muskmelon peel/H_2SO_4	$ZnFe_2O_4$/AC composite	500 °C, 2 h, 1.5:1 H_2SO_4/ precursor	82.91	0.021	2.580	C, N, O, Zn, Fe, pH_{PZC} 7.24	[97]
Coal/commercial	Fe_2O_3/AC composite		1012.0	0.649	1.283	pH_{PZC} 5.0	[98]
Coal/commercial	Raw AC		922.0	0.614	1.284	pH_{PZC} 6.9	[98]
Commercial	Zeolite 5 A/AC composite		728.6	0.342			[99]
Soya bean husk/H_2SO_4	Zr^{4+} embedded chitosan/AC composite	500 °C, 1 h, 2:1 H_2SO_4/precursor, 50 °C/min	147.85	0.227	7.324	C53.73, N 6.43, O 34.67, Cl 3.68, Zr 1.49	[100]
Pine cone/H_3PO_4	Zero valent iron/AC composite	500 °C, 1 h, 3:1 H_3PO_4/ precursor, 25 mL/min N_2, 8 °C/min	350.8			C 82.45, H 2.03, O 8.12, N 2.96, ash 4.17 %	[101]
Commercial	Polyaniline/AC composite		260.5	0.280	4.23	C 82.93, N 8.28, O 7.03, P 0.43, Cl 1.13, Fe 0.20	[46]
Coal fine slag/HCl	Silica/AC composite	600 °C, 3.5 h, 21.8 % HCl	335.0	0.338	5.355	C 43.74	[102]

S_{BET}: BET surface area; V_t: total pore volume; d_p: average pore size; C: carbon; H: hydrogen; O: oxygen; N: nitrogen; pH_{PZC}: point of zero charge.

developed after modification [61]. For this purpose, several modifications including acid, alkali, surfactant, magnetic, urea, amines, $ZnCl_2$, and others (Table 1) were used to modify AC-based adsorbents in order to optimize the nitrate removal performance [62–82].

Acid modification of carbon is commonly used to oxidize the surface of porous carbon as it enhances the acidic characteristic or acidic groups (i.e., oxygenated groups with proton donors) and, eliminates the inorganic elements and affects the surface hydrophilicity [83]. Nitric and sulfuric acids are most extensively used for this purpose along with some other acids. Acid treatment was adopted to modify the surface and pore characteristics of a commercial AC [62]. First, ash was eliminated from AC, and the oxidation and outgassing steps were performed as follows: AC was rinsed with hydrochloric acid followed by fluoric acid to eliminate ash from the carbon structure, frequently boiled with distilled water until constant pH, and dehydrated in oven at 110 °C. The ash content was declined from 5.5 % to 0.33 % after the de-ashing step, and no affecting minerals for nitrate adsorption could be found in the ash. The de-ashed AC was also treated with 8 M HNO_3 solution for 6 h at 95 °C, frequently rinsed with distilled water, and calcined in air for 4 h at 350 °C for complete decomposition of residual acid. The oxidized carbon was further outgassed at 900 °C to eliminate strong functional groups such as carboxyl and lactonic groups and was denoted as Ox-9OG AC. The pore properties, C and O contents, and acidic and basic group contents of de-ashed AC were 1146 m^2/g and 0.612 cm^3/g, 90.84 % and 8.51 %, and 0.60 and 0.29 meq/g, respectively. After HNO_3 modification these characteristics were 815 m^2/g and 0.406 cm^3/g, 80.16 % and 18.80 %, and 2.61 and 0.06 meq/g, respectively. Both surface area and pores volume were declined; meanwhile oxygen content was considerably enhanced for oxidized carbon. The content of total acidic groups identified by Boehm titration was also enhanced after oxidation. The adsorption performance of Ox-9OG AC was 1.5 times more than that of de-ashed AC. Ox-9OG AC had the highest Langmuir capacity and affinity extent for nitrate adsorption despite its smaller surface area. The reason might be related to the existence of strong basic groups such as positively charged quaternary nitrogen on Ox-9OG AC which could efficiently attract NO_3^- anions. This behavior suggested that the surface properties had a significant role in NO_3^- removal by AC compared to the pore properties [68].

Base (alkaline) treatment of AC can develop the porous structure which results in a high adsorption performance towards nitrate. In this regard, Mazarji et al. [63] modified coconut shell/steam-AC with sodium hydroxide as follows: AC was pretreated by washing repeatedly

with warm distilled water to remove soluble species, and oven dried at 60 °C overnight. Then, it was treated with 1.25 M NaOH solution under stirring for 7 h at 75 °C. The sample was then sequentially rinsed with 0.5 M HCl and distilled water until elimination of all the salts. After that, the obtained sample was oven dehydrated at 60 °C overnight. Modified AC exhibited BET surface area, total pore volume, and micropore volume of 901 m^2/g, 0.490, and 0.400 cm^3/g compared to 888 m^2/g, 0.480, and 0.376 cm^3/g for raw AC. The morphology of the ACs showed that the NaOH modification had developed the microporous structure of carbon. It could be due to the role of alkali in decomposition of some structural species in the coconut shell; thereby, the NaOH modified AC exhibited a clean surface relative to the raw AC. The high microporosity may be favorable for nitrate removal [75]. Furthermore, NaOH might solubilize most of the organic materials in water by reducing the interaction forces between adsorbate and carbon surface, hence preventing them from interfering with nitrate adsorption. Consequently, the removal efficiencies of modified and raw ACs for nitrate ions were 17 % and 7.5 %, respectively. FTIR spectra of the raw and treated ACs displayed a slight shifting in the positions of OH, C−O, and C═C functional groups. This indicated that the NaOH modification did not considerably alter the peaks' positions of the raw AC relative to modified AC.

Surfactants treatment enhances the surface hydrophobicity and can also provide the positively charged functionality which aids in the adsorption of anionic species in greater quantities. Cationic surfactants were extensively applied for treatment of AC-based adsorbents. In this regard, Allalou et al. [84] treated date stems/$ZnCl_2$-derived AC with cationic cethyl trimethyl ammonium bromide (CTAB) surfactant, as follows: Raw AC was added to 100 mL of 30 mmol/L of CTAB solution and the mixture was agitated at 25 °C for 4 h. Modified AC was then filtered, rinsed with distilled water, and dehydrated at 105 °C. BET surface area of AC was declined from 1407 up to 569 m^2/g after surfactant modification, indicating the aggregation of ammonium groups on the external surface of AC. FTIR spectrum of the treated AC showed two novel bands in terms of tertiary amine and methyl (CH_2) groups, which are not appeared in the spectrum of raw AC. These observations confirmed that CTAB was submitted onto the structure of modified AC. Consequently, an enhancement in nitrate adsorption from 14 % on the raw AC to 60 % on the CTAB-AC was reported. The head group of cationic surfactant (CTA^+) was adsorbed on the AC surface and provided additional positive active sites. Thus, nitrate anions were attracted on CTA^+ and their removal was improved [80]. The scanning electron microscope (SEM) morphology showed a rough surface for the raw date stems with no pores. Meanwhile, AC exhibited a heterogeneous and porous structure. The porous structure of the AC surface was formed by the $ZnCl_2$ evaporation during the activation step, which resulted in a larger surface area (1407 m^2/g). Similar results were observed for the treatment of commercial AC by cationic surfactant, cetyltrimethyl ammonium chloride (CTAC) [64]. The modified AC had surface area, total pore volume, and average pore radius of 926.80 m^2/g, 0.589 cm^3/g, and 0.599 nm compared to 1359.6 m^2/g, 0.809 cm^3/g, and 0.549 nm for virgin AC. The decrease in pore properties of AC after modification was due the partial existence of CTAC molecules in micropores of AC which resulted in the blockage of pores. SEM images of virgin and modified ACs showed the appearance of some brighter area on the surface of modified AC relative to virgin AC which verified the presence of the CTAC molecules on the surface of AC. Adsorption performance of modified AC towards nitrate was about 3 (2.8) times more than that of virgin AC. The results confirmed that the CTAC treatment favorably affects the performance of AC adsorbent towards nitrate. This could be related to the electro-attraction of the nitrate anions towards active cationic adsorption sites of CTAC modified AC [58].

Magnetization has been considered as a promising way to enhance the functionality of AC adsorbent and also can develop its porous structure. For this purpose, iron materials such as $FeCl_3$, $FeSO_4$, Fe_3O_4, and others represent the common applied magnetic agents. For instance, Tan et al. [65] obtained magnetic corn straw/H_3PO_4 derived AC by using $FeCl_3$ as magnetic agent. In brief, 5 g of AC was mixed with $FeCl_3$ solutions (consisting of 40 g $FeCl_3$.6 H_2O/ 500 mL ultrapure water) for 24 h under stirring, and then oven-dehydrated for 12 h at 105 °C. BET surface area of magnetic AC (217.87 m^2/g) declined compared to raw AC (563.93 m^2/g). This result could be related to the iron complex which blocked the inner pores [67,85]. However, the O/C and (O + N)/C ratios considerably enhanced to 0.281 and 0.291 for magnetic AC as compared to 0.154 and 0.144 for raw AC, respectively, indicating the enhancement of oxygenated groups. FTIR patterns of the AC adsorbents showed that the intensity of C–O and –OH peaks insignificantly enhanced for magnetic AC in comparison with raw one. In addition, the Fe–O band was observed in the magnetic adsorbents. These findings confirmed that the surface functionality of adsorbents were changed after modification and the oxygenated groups were enhanced (i.e. C–O

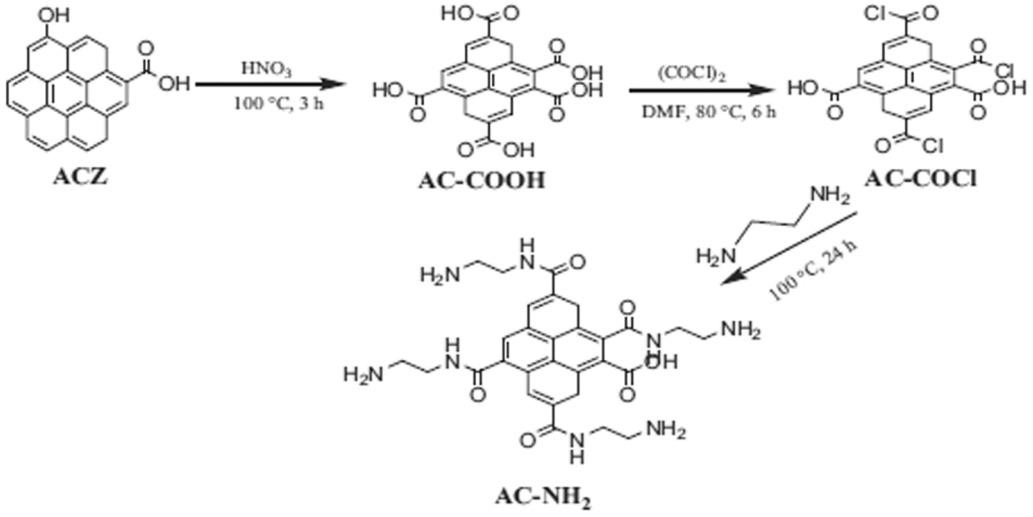

Fig. 1. Scheme of the synthesis steps of amino-functionalized Naudin seed shells AC [71].

and –OH). The zeta potentials of all magnetic adsorbents considerably changed toward larger pH relative to raw AC, suggesting the development of positive charges at the magnetic AC surface. Therefore, the adsorption performance of magnetic AC towards NO_3^- was 1.6 times more than that of raw AC due to the enhanced attraction between anionic NO_3^- and positive charges of magnetic AC surface. The magnetic modification can also increase the surface area of AC, as explained by Arbabi et al. [66] for the modified almond shells/H_3PO_4 derived AC by magnetic Fe^{3+}/Fe^{2+} solution. BET surface area of modified AC was more than twice that of raw AC, which might be related to the fact that iron particle was reacted with carbonaceous material within the pyrolysis [65,86]. Modified AC had an elemental content of 44.42 % C, 32.77 % O, and 19.66 % Fe. Moreover, the FTIR spectrum of magnetic AC showed a strong peak for iron bonds Fe-O. This resulted in a favorable adsorption of nitrate ions due to the developed porosity and functionality of modified AC structure.

Nitrogen-enriched groups commonly impart the basicity to surface, which improves the attraction extent of porous carbon for anionic species. Treatment with urea, ethylenediamine and 3-aminopropyl trimethoxysilane has been adopted for producing ACs with basic surface properties and high performance towards nitrate. For instance, Nunell et al. [68] modified pine cones/H_3PO_4-derived AC by saturated urea solution. Urea modified ACs exhibited a greater nitrogen content (13.0 %) relative to that of the unmodified sample (0.4 %), along with an enhancement in pH and pH_{PZC} values (from 3.8 & 5.1–4.5 & 6.0), meanwhile a decline in ash and carbon contents (1.6 % and 67.0 % relative to 4.1 % and 88.2 %) were evidenced for those ACs. Modified ACs showed 1.6 meq/g acidic oxygen groups and 0.5 meq/g basic surface functional groups compared to 1.7 meq/g acidic oxygen-containing groups with no basic groups for raw AC. In turn, urea treatment resulted in the development of basicity which could be related to the existence of nitrogen-containing groups such as amino and/or amidine groups. Consequently, the performance of urea treated AC adsorbent was about 3 times more than that of raw AC. Similar results were observed for the amino-functionalized *Cucumerupsi manni* Naudin seed shells/$ZnCl_2$ AC by using ethylenediamine (EDA) as modifying agent [71] and amino functionalized sucrose/H_2SO_4 AC by using 3-aminopropyl trimethoxysilane [72]. The amino-functionalized Naudin seed shells AC was produced by oxidation followed by acyl chlorination and amidation steps, as schematically presented in Fig. 1. All of these post-treatment resulted in an enhancement in the adsorption performance towards nitrate despite a noticeable reduction in the pore properties of the AC, probably due to the blockage of small pores by nitrogen species [71,87]. These observations indicate the significant role of the surface chemistry in nitrate removal by ACs. In particular, some basic oxygenated species along with N-containing groups, such as amidine and/or amino groups, could act as selective active sites for nitrate ions. Moreover, basic sites released from p-electrons on the graphitic like layers could receive specific protons leading to a positively charged surface and a noticeable raise in the adsorbed amount [70].

The literature also included the use of other chemicals such as $ZnCl_2$ [59,73,74], Zn, $ZnSO_4$ [78], quaternary ammonium-based polymer [88], H_2O_2 [89], and $CaCl_2$ [90,91] to modify AC-based adsorbents for removing nitrate. All of these chemicals resulted in an enhancement in the content of positively charged active sites in the structure of AC-based adsorbents which favored the attraction of anionic nitrate. For instance, Bhatnagar et al. [59] observed that the performance of $ZnCl_2$ modified coconut AC adsorbent towards nitrate was enhanced up to 6 fold relative to unmodified AC. The reason was due to the presence of some zinc oxide in the form of a needle like structure (Fig. 2) in macro- and mesopores of AC which favored the adsorption of nitrate anions. Other chemicals such as $KMnO_4$ [61,77] exhibited an enhancement in the total pore volume and BET surface area.

Chemical treatments have been widely applied for modifying the functionality and porosity of the AC-based adsorbents structure to improve adsorption efficiency. Nevertheless, a single treatment step may not be highly effective due to its specific role. Thus, the use of two or more combined treatment steps from different methods can provide the benefits of combining the merging the particular advantages of these steps [92].

In this regard, the alkali treatment has been extensively applied as an essential step in the combined treatment of AC-based adsorbents. This step enhances the reactivity of the carbon structure for further treatment steps. For instance, Mazarji et al. [63] sequentially modified coconut shell-AC with NaOH and a cationic cetyl trimethyl ammonium bromide (CTAB) surfactant to enhance its performance for the removal of nitrate from water. The values of BET surface area, micropores volume, and total pores volume for raw AC were 888 m^2/g, 0.376 cm^3/g, and 0.480 cm^3/g. These characteristics were 901 m^2/g, 0.400 cm^3/g, and 0.490 cm^3/g for alkali modified AC relative to 722 m^2/g, 0.310 cm^3/g, and 0.420 cm^3/g for alkali-CTAB modified AC. The alkali modification develops the microporosity of AC structure. It could be related to the role of alkali in decomposition of some structural species of the coconut shell. The low BET surface area of two-steps modified AC might be due to the complete filling of some micropores with CTAB which resulted in a lowest micropore volume relative to other adsorbents [64]. FTIR spectra showed that two-steps modified AC had a variety of surface groups including –OH, C–C, C–O, and C–X groups. Moreover, a significant $–CH_2$ group was also found which related to the CTAB loaded on two steps modified AC. High removal percentage of approximately 80 % was reported for nitrate on two steps treated AC compared to 7.5 % on raw AC and 17 % on alkali modified AC at an initial nitrate amount of 40 mg/L, adsorbent dosage of 4 g/L, and 25 °C. The two steps modified AC exhibited the best performance relative to others in spite of its smallest micropore volume and surface area. This result indicated that the extent and type of active groups on AC surface had an essential role in nitrate removal [58]. In particular, the quaternary ammonium groups

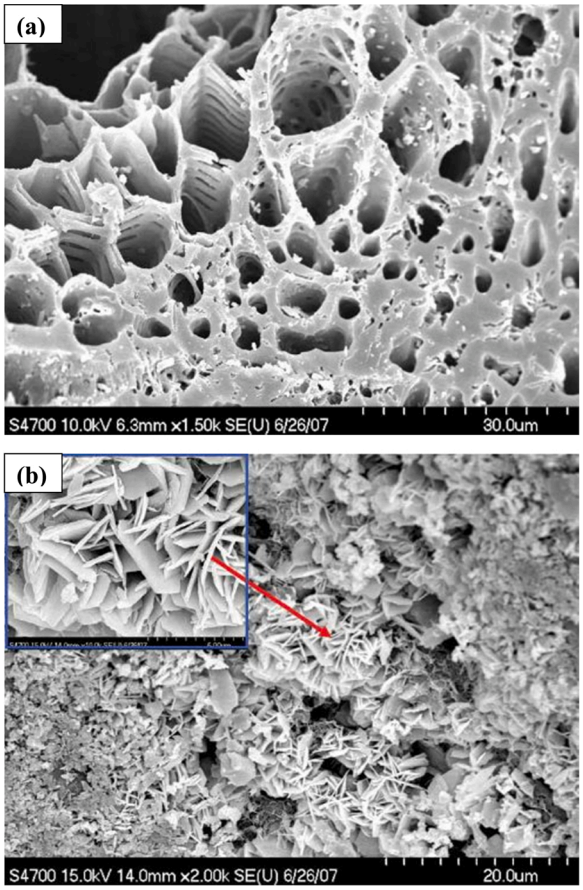

Fig. 2. SEM images of (a) untreated and (b) $ZnCl_2$ treated coconut AC [59].

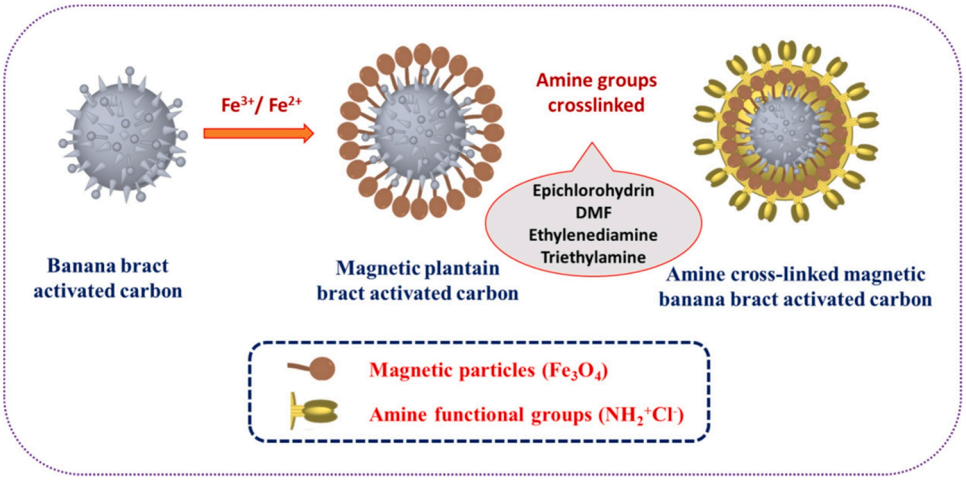

Fig. 3. Synthesis route of magnetic amino functionalized banana bract AC [82].

left on the AC surface after CTAB treatment, led to enhance the positive charges and improve the attraction extent for the anionic nitrate.

Similar results were observed for the treatment of vetiver grass/KOH derived AC by combined metal salt and cationic surfactant steps using zirconium chloride octahydrate ZR, cetyltrimethyl ammonium bromide CTAB, respectively [80]. The BET specific surface area, total pore volume, and average aperture for raw AC were 1379.63 m^2/g, 0.711 cm^3/g, and 2.060 nm; for ZR modified AC were 1245.38 m^2/g, 0.617 cm^3/g, and 1.980 nm; for ZR/CTAB modified AC were 222.95 m^2/g, 0.191 cm^3/g, and 3.423 nm. The pore volume and surface area of ZR/CTAB/AC were highly declined because CTAB and ZR were submitted into the structure of AC; causing the blockage of pores. Nevertheless, ZR/CTAB/AC was obstructed greater than ZR/AC. The removal efficiency of nitrate by ZR/CTAB modified AC was 44.92 % compared to 5.32 % and 5.73 % for raw AC and ZR modified AC, respectively. This confirmed that raw AC had little influence on the nitrate removal. The performance of ZR/CTAB/AC adsorbent was considerably enhanced in spite of the significant decline in its BET surface area. Cationic surfactants are widely utilized to enhance the number of positive charges on the AC surface to improve its ability for the adsorption of inorganic anions like nitrate [84]. FTIR spectra showed that ZR/CTAB/AC structure exhibited numerous surface groups such as –COO and C–H which played an essential role in the removal of contaminants. Functional groups enriched structure was also observed for magnetic amino functionalized banana bract/H_2SO_4 AC synthesized via combined magnetization and amine-crosslinked steps (Fig. 3). Several groups including Fe–O, F–OOH, C–N, and –NH_2 were introduced into the structure of AC which favored the adsorption of nitrate [82].

3.3. Activated carbon composite

A composite consists of a developed structure of two or more components, which provides activity and support [93]. Moreover, these composites can exhibit favorable adsorption capability owing to their

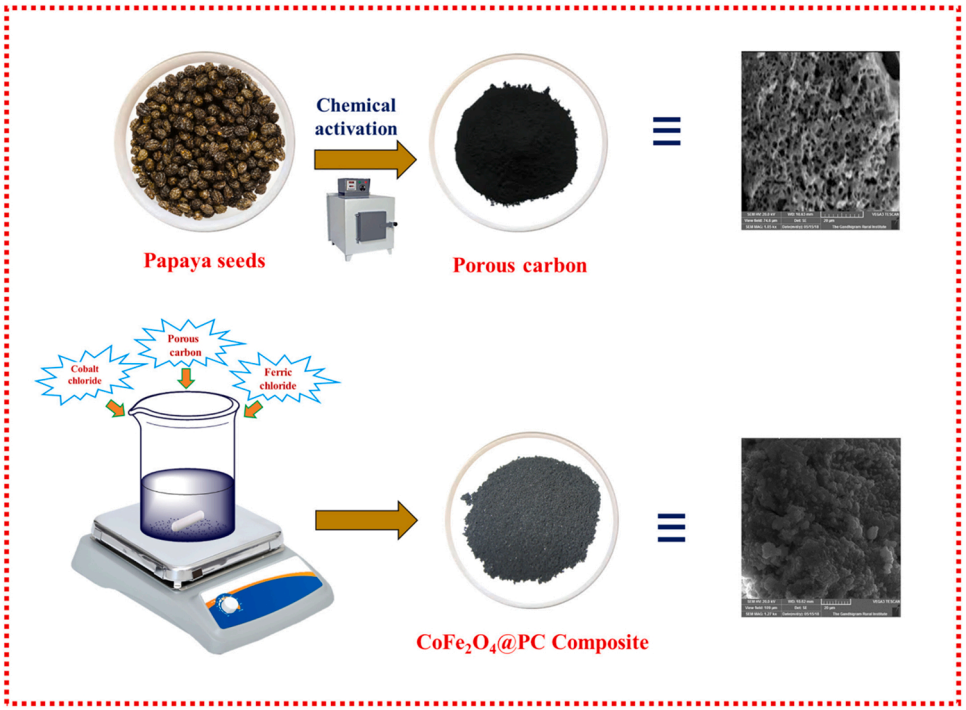

Fig. 4. Synthesis route of $CoFe_2O_4$/ papaya seeds derived AC composite [105].

improved functionality and porosity [94]. In the literature [95–102], various materials were used for the preparation of AC composite adsorbents such as layered double hydroxides (LDHs), Fe_2O_3 nanoparticles, zeolite, chitosan, and others (Table 1).

LDHs have a favorable structure with large porosity and more positively charges. Thus, the introducing of LDHs into AC can improve its surface charge and adsorption performance for anionic nitrate [95]. In this regard, Mg/Al-LDHs AC composite was prepared by co-precipitation process, as follows: Apple branch-biochar was added to 500 mL of 0.03 M $MgCl_2$ and 0.01 M $AlCl_3$ solution (3:1 Mg/Al ratio). The mixture was then treated by 40 kHz ultrasonic dispersion for 6 h and stirred for 6 h. The pH value of the sample was set to 8–9 by 0.2 M NaOH and 0.3 M Na_2CO_3 solutions. The obtained black sample (Mg/Al-LDHs with biochar) was placed in a Teflon autoclave and exposed to a hydrothermal treatment for 4 h at 120 °C, then filtered and rinsed repeatedly with deionized water. After that, the solid sample was introduced into a muffle furnace and exposed to calcination under CO_2 flow for 1 h at 500 °C to produce Mg/Al-LDHs AC composite which was denoted as AMB [60]. S_{BET} and total pore volume as well as average pore width were 257.64 m^2/g, 0.161 cm^3/g, and 6.25 nm for AMB compared to 526.34 m^2/g, 0.437 cm^3/g, and 3.29 nm for AB. Thus, the pore volume and S_{BET} of AMB declined while the average pore width enlarged relative to AB, which indicated that the loaded Mg/Al-LDHs had filled the voids on the surface of AC [103]. The enlargement in pore width of AC might be due to the higher pore width of the Mg/Al-LDHs. The elemental contents were 43.71 % C, 1.97 % H, 14.60 % O, 0.65 % N, 15.76 % Mg, and 6.24 % Al for AMB relative to 80.96 % C, 1.81 % H, 10.68 % O, 1.42 % N, 0.87% Mg, and 0.94 % Al for AB. Clearly, the contents of C and N for AMB were considerably smaller than those for AB, while the contents of O, H, Mg, and Al for AMB were larger, suggesting the well modification of the AB surface with the Mg/Al-LDHs. Since the later contains Mg^{2+} and Al^{3+} as well as —OH, after the loading of Mg/Al-LDHs on the AB surface, the extents of these elements enhanced and the content of C declined. The values of pH and CEC were 9.17 and 126.31 cmol/kg for AMB relative to 8.12 and 64.82 cmol/kg for AB. The higher values of pH and CEC for AMB relative to those for AB indicated the specific characteristics of AB and Mg/Al-LDHs materials in a composite because Mg/Al-LDHs had alkaline and interlayer ion exchange natures [96]. The FTIR spectrum of AMB showed that relative to AB, the intensities of the —COOH and —OH groups were considerably increased, which confirmed the attachment of the Mg/Al-LDHs to the surface of AB. Furthermore, the peak extent of C═O groups was obviously reduced for AMB relative to AB due to the consumption of these groups and the formation of metal-oxygen bonds during interlayer anion calcination [104]. This was clearer in AMB, where combination with the Mg/Al-LDHs provided more positively charged active sites on the surface, which enhanced the NO_3^- adsorption. The average uptake of AMB for NO_3^- is 7.43 times that of AB, and the average adsorption rate for NO_3^- increased from 13 % to 83 %.

Magnetic materials such as iron oxides in terms of Fe_2O_3 or Fe_2O_4 can be introduced into the AC structure to obtain a composite adsorbent which will merge the large uptake of composite and the separation capability of magnetic compounds [97]. The iron oxide offers a high extent of adsorption sites and comparatively improves the pore properties of the adsorbent [105]. Thus, magnetic AC composites have received the interest of numerous researchers as adsorbents with easier separation and high removal efficiency for nitrate pollutant. Mehrabi et al. [98] prepared Fe_2O_3/ coal-derived AC composite by contacting raw AC with 140 mL of 3 M $FeCl_3$ at 56 °C for 48 h under stirring at 180 rpm. Then, the composite rinsed with deionized water frequently until the filtrate reached a fixed pH as well as no detected iron. The composite was then oven dehydrated at 100 °C overnight. The BET, total pore volume, average pore radius, and pH_{PZC} were 1012 m^2/g, 0.649 cm^3/g, 12.83 Å, and 5.0 for Fe-AC relative to 922 m^2/g, 0.614 cm^3/g, 12.84 Å, and 6.9 for AC. According to results, modification enhanced the pore volume and surface area, which could relate to the removal of impurities from the structure of AC. Furthermore, pH_{PZC} of Fe-AC was declined relative to AC which suggested more positive charge on the composite adsorbent. The FTIR spectra exhibited a raise in the extent of Fe-O-H group in Fe-AC composite relative to AC which affirmed the existence of more. Moreover, a new Fe-O group was observed in Fe-AC structure. These functional Fe- containing groups confirmed that Fe_2O_3 nanoparticles were efficiently loaded on AC surface [65]. The elemental analysis showed that Fe-AC structure consisted of 16.8 % Fe which affirmed the effective coating of iron on AC. SEM results showed that Fe-AC had fewer impurities relative to the AC which indicated their removal after the modification. From the Langmuir model, maximum uptakes were 17.7305 and 11.0132 mg/g for Fe-AC and AC, respectively. The removal efficiency was also considerably improved from 63.8 % to 91.3 %. The results revealed that the composite adsorbent had large performance for the removal of nitrate relative to AC adsorbent. Development of nitrate removal was due to the influence of treatment with iron materials that rinsed impurities and enhanced the positive charges of AC with Fe^{3+}. These charges resulted in a large affinity towards nitrate anions [81]. Another team by Karthikeyan et al. [105] prepared $CoFe_2O_4$/ papaya seeds derived AC composite according to the synthesis route presented in Fig. 4. The composite showed high adsorption performance towards nitrate owing to its favorable functionality and porosity.

Zeolite /AC composite has excellent cation exchange capacity and superior adsorption capacity due to zeolite and activated carbon. Hong & Suh [99] evaluated the possibility of nitrate removal from water using the zeolite/AC composite. The composite or zeocarbon consisted of a blend of zeolite 5 A and AC. HCl pretreatment was performed for this composite in order to enhance its mechanical and structural properties. The performance of zeocarbon (surface area 728.6 m^2/g) for nitrate removal was compared with an acid pretreated commercial AC (surface area: 850 m^2/g) and zeolite 5 A (surface area: 550 m^2/g). The adsorption performance was 55.5 % for zeocarbon compared to 0 % for zeolite and 64.5 % for AC. Zeolite showed no removal for nitrate, meanwhile AC exhibited high adsorption performance owing to its large surface area [49]. On the other hand, the treated zeocarbon also showed high adsorption performance toward nitrate relative to the commercial adsorbents. This behavior could be related to the fact that the zeocarbon had the properties of ion exchange by Ca^{2+} and adsorption capability of zeolite and AC, respectively.

Chitosan is a cost-effective, quite abundant, and eco-friendly biopolymer. It has a structure of large pore size and large extent of amino and hydroxyl surface groups. Thus, incorporation of chitosan into AC structure can further improve the functionality of AC and its performance for attracting pollutants of large molecules [94]. Moreover, incorporation of AC into the structure of chitosan is an effective step to enhance its mechanical strength and thermochemical stability. CS-AC structure has the advantages of porous nature and preferable strength. In this regard, Banu et al. [100] prepared Zr^{4+} ions modified chitosan-soya bean husk/H_2SO_4 AC composite for nitrate removal, as follows: 10 g of chitosan was uniformly dissolved in 500 mL of 2 % acetic acid solution, mixed with 5 g of AC, and continually agitated for 5 h to produce a homogenous sample of AC dispersed in the chitosan gel. CS-SAC composite was formed by dropping the dispersed sample into the 1 M NaOH solution and was left for 24 h. The composite was then rinsed repeatedly with distilled water until the filtrate had pH 7. The wet composites were exposed to cross-linking with 2.5 wt% glutaraldehyde solution, immersed in 5 % $ZrOCl_2{\cdot}8\ H_2O$ solution for 24 h to produce Zr^{4+} ions modified CS-SAC composites, and rinsed twice with distilled water to eliminate surplus free ions. The sample was then dehydrated at room temperature to produce Zr-CS-SAC composite. FTIR spectra of Zr-CS-SAC exhibited the Zr−N and Zr-O-C groups which confirmed that Zr^{4+} ions were loaded onto the composite. Around 38.2 mg/g uptake of nitrate was reported in 45 min on Zr-CS-SAC. Meanwhile, for CS-SAC the nitrate uptake was 24.2 mg/g indicated that the removal performance of Zr-CS-SAC was higher than CS-AC which could be related to higher

Table 2
Isotherm study conditions and results of nitrate ions removal using different AC-based adsorbents.

Precursor/activator	Adsorbent	Isotherm conditions	q_{max} (mg/g)	Isotherm	Ref.
Finnish wood chips/CO_2	Raw AC	5 g/L, rT, 24 h, pH 4, 10–140 mg/L	11.198	Langmuir	[45]
Coconut shells/ Steam	Raw AC	5 g/L, rT, 24 h, pH 4, 10–140 mg/L	14.599	Langmuir	[45]
Olive jift/$ZnCl_2$	Raw AC	20 g/L, 20 °C, 24 h, pH 4, 100–300 mg/L	5.525	Langmuir	[118]
Sugar beet bagasse/$ZnCl_2$	Raw AC	2 g/L, 45 °C, 6 h, pH 6.58, 10–200 mg/L	27.55	Langmuir	[51]
P. aculeate sawdust/H_3PO_4	Raw AC	10 g/L, 25 °C, h, pH 2, 0.1–6 mmol/L	6.82	Langmuir	[70]
P. aculeate sawdust/KOH	Raw AC	10 g/L, 25 °C, h, pH 2, 0.1–6 mmol/L	18.60	Langmuir	[70]
Finnish wood chips/$ZnCl_2$	Raw AC	5 g/L, rT, 24 h, pH 6, 25–125 mg/L	80.0	Langmuir	[55]
P. juliflora branches/H_2SO_4	Raw AC	1 g/L, 30 °C, 1 h, pH 6.7, 1–100 mg/L	10.989	Langmuir	[52]
Sugar cane bagasse/ H_3PO_4	Raw AC	10 g/L, 25 °C, 0.5 h, pH 4, 5–40 mg/L	18.502	Freundlich	[119]
Coconut/commercial	Raw AC	10 g/L, 20 °C, 12 h, pH n, 5–100 mg/L	0.28	Freundlich, Langmuir	[73]
Commercial	Raw AC	66.7 g/L, 20 °C, 1 h, pH 6.5, 50–175 mg/L	0.542	Freundlich	[120]
Orange peel/H_3PO_4	Raw AC	g/L, °C, h, pH 2, 0.05–8 mmol/L	18.91	Langmuir	[47]
Almond shells/steam	Raw AC	g/L, °C, h, pH 2, 0.05–8 mmol/L	55.56	Langmuir	[47]
Oil palm shells/H_3PO_4-steam	Raw AC	5 g/L, rT, 80 min, pH 2, 20–100 mg/L	65.488	Langmuir	[48]
Oil palm shells/KOH-steam	Raw AC	5 g/L, rT, 80 min, pH 2, 20–100 mg/L	68.166	Langmuir	[48]
Rice husk/NaOH	Raw AC	2 g/L, 20 °C, 3 h, pH, 50–400 mg/L	86.20	Redlich-Peterson, Langmuir	[49]
Sucrose	Raw AC	0.24–0.96 g/L, 21 °C, 10 h, pH 7–8, 2 mg/L	7.98	Freundlich, Langmuir	[121]
Bituminous coal/commercial	Raw AC	0.24–0.96 g/L, 21 °C, 10 h, pH 7–8, 2 mg/L	6.38	Freundlich, Langmuir	[121]
Coal/commercial	Raw AC	6.5 g/L, 25 °C, 24 h, pH 3, 25–200 mg/L	11.01	Langmuir	[98]
Bituminous coal/commercial	Raw AC	2 g/L, °C, 24 h, pH 4, 0.1–1.0 mmol/L	17.98	Langmuir	[122]
G. globra residues/$ZnCl_2$	Raw AC	4 g/L, 35 °C, 90 min, pH 2, 20–100 mg/L	142.58	Langmuir	[56]
Shrimp shell/$ZnCl_2$	Raw AC	2.5 g/L, 25 °C, 10 min, pH 3, 10–150 mg/L	10.0	Langmuir, Freundlich	[54]
Coconut shell/commercial	Raw AC	6.7 g/L, 30 °C, 20 h, pH 4, 0–450 mg/L	16.49	Langmuir	[123]
P. aculeate trunks /K_2CO_3	Raw AC	10 g/L, 25 °C, 300 min, pH 2, 0.1–6.0 mmol/L	21.08	Langmuir	[57]
P. aculeate trunks /NH_4Cl	Raw AC	10 g/L, 25 °C, 30 min, pH 2, 0.1–6.0 mmol/L	24.80	Freundlich	[57]
Coir pith/$ZnCl_2$	Raw AC	4 g/L, 35 °C, 20 min, pH 3, 10–40 mg/L	10.3	Langmuir, Freundlich	[50]
C. carandas stems/H_2SO_4	Raw AC	1.3 g/L, 30 °C, 50 min, pH 7, 10–150 mg/L	55.56	Langmuir	[113]
Pomegranate peel/ H_3PO_4 +$ZnCl_2$	Raw AC	5–80 g/L, 20 °C, 45 min, pH 7.2, 50–400 mg/L	78.125	Langmuir	[114]
Pine cones/H_3PO_4	Urea modified AC	10 g/L, 25 °C, pH 2, 0.1–8 mmol/L	27.90	Langmuir	[68]
Pine cones/H_3PO_4	Raw AC	10 g/L, 25 °C, pH 2, 0.1–8 mmol/L	9.92	Langmuir	[68]
Rice husk/K_2CO_3	Urea modified AC	1 g/L, 25 °C, 24 h, pH, 5–15 mg/L	8.10		[69]
Coconut shell	NaOH-CTAB modified AC	4 g/L, 25 °C, 2 h, pH 7, 40–200 mg/L	21.51	Langmuir	[63]
Commercial	HNO_3 modified AC	2 g/L, 25 °C, 24 h, pH n, 0.15–3.3 mmol/L	13.02	Langmuir	[62]
Corn straw/ H_3PO_4	$FeCl_3$ modified AC	0.83 g/L, 25 °C, 24 h, pH 6, 0.5–50 mg/L	2.06	Freundlich	[65]
Corn straw/ H_3PO_4	Raw AC	0.83 g/L, 25 °C, 24 h, pH 6, 0.5–50 mg/L	1.28	Langmuir	[65]
Polyacrylonitrite fiber/ $ZnCl_2$	Quaternary nitrogen modified AC	2 g/L, rT, 12 h, pH 3, 10–400 mg/L	57.66	Langmuir	[76]
Sucrose/H_2SO_4	Amino modified AC	3 g/L, 25 °C, 1 h, pH 7, 50–250 mg/L	48.78	Langmuir	[72]
Strip moso bamboo/H_3PO_4	quaternary nitrogen modified AC	2 g/L, rT, 12 h, pH 3, 0–200 mg/L	28.52		[75]
Lignite	Cationic polymer modified AC	2.5 g/L, 23 °C, 4 h, pH 6.65, 25–376 mg/L	27.56	Langmuir	[88]
Lignite	Raw AC	2.5 g/L, 23 °C, 4 h, pH 6.65, 25–376 mg/L	14.25	Langmuir	[88]
Banana bract/H_2SO_4	Amine/Fe_3O_4 modified AC	2 g/L, 30 °C, 1.5 h, pH 7, 50–150 mg/L	75.815	Freundlich	[82]
Coal/commercial	NH_3 modified AC	2 g/L, 25 °C, 12 h, pH 5, 100–800 mg/L	31.40	Langmuir	[124]
Coal/commercial	Raw AC	2 g/L, 25 °C, 12 h, pH 5, 100–800 mg/L	13.50	Langmuir	[124]
Coconut/commercial	$ZnCl_2$ modified AC	10 g/L, 20 °C, 12 h, pH n, 5–100 mg/L	14.01	Freundlich, Langmuir	[73]
Almond shell/commercial	$FeSO_4$ modified AC	g/L, 20 °C, 2 h, pH 6.2, 0–20 mg/L	20.0		[125]
Commercial	$CaCl_2$ modified AC	10 g/L, 25 °C, 1 h, pH 6, 5–40 mg/L	1.791	Langmuir	[90]
Lignite/commercial	$ZnCl_2$ modified AC	10 g/L, 25 °C, 24 h, pH 5, 5–150 mg/L	10.85	Langmuir, Freundlich	[74]
Coconut shell/steam	$ZnCl_2$ modified AC	10 g/L, 25 °C, 2 h, pH 5.5, 5–200 mg/L	10.26	Langmuir	[59]
Commercial	$CaCl_2$ modified AC	20 g/L, 25 °C, 2 h, pH 6, 10–20 mg/L	1.931	Redlich-Peterson	[91]
Date stems/$ZnCl_2$	Surfactant modified AC	3 g/L, 25 °C, 0.5 h, pH 5.8, 100–600 mg/L	83.33	Langmuir, Freundlich	[84]
Grape wood/H_2SO_4	Iron modified AC	6 g/L, 25 °C, 72 h, pH 4, 25–150 mg/L	55.82	Langmuir	[67]
Grape wood/H_2SO_4	Raw AC	6 g/L, 25 °C, 72 h, pH 4, 25–150 mg/L	37.51	Freundlich	[67]
C. manni naudin shells/$ZnCl_2$	Amine modified AC	1 g/L, 27 °C, 50 min, pH 3, 50–200 mg/L	192.92	Freundlich	[71]
Almond shells/H_3PO_4	Magnetic AC	0.5 mg, °C, 20 min, pH 4, 25–400 mg/L	58.47	Langmuir	[66]
Vetiver grass/KOH	ZR/CTAB modified AC	6 g/L, 25 °C, 120 min, pH 3, 20–40 mg/L	5.365	Freundlich	[80]
Commercial	CTAC modified AC	2.5 g/L, 25 °C, 30 min, pH 7, 10–150 mg/L	10.80	Freundlich	[64]
Commercial	Fe_3O_4 modified AC	1 g/L, 20 °C, 60 min, pH 3, 50–300 mg/L	57.1	Langmuir	[85]
Rice straw/steam	$KMNO_4$ modified AC	4 g/L, 25 °C, 24 h, pH 3–9, 50 mg/L	19.70	Langmuir- Freundlich	[61]
Commercial	$FeCl_3$ modified AC	15 g/L, °C, 45 min, pH 7, 50–300 mg/L	28.90	Langmuir	[126]
Commercial	Fe^{2+}, H_2O_2 modified AC	1.5 g/L, 25 °C, 2 h, pH 4, 10–50 mg/L	43.10	Freundlich	[81]
Petroleum pitch/commercial	$(NH_4)_2S_2O_8$ Modified AC	2 g/L, °C, h, pH 2.5, 0.81–6.45 mmol/L	0.58	Langmuir	[79]
Petroleum pitch/commercial	Raw AC	2 g/L, °C, h, pH 2.5, 0.81–6.45 mmol/L	0.40	Langmuir	[79]
Coal fine slag	Silica/AC composite	2.5 g/L, 20 °C, 10 h, pH 6, 5–35 mg/L	11.45	Langmuir	[102]
Soya bean husk/H_2SO_4	Zr^{4+} embedded chitosan/AC composite	2 g/L, 30 °C, 45 min, pH 7, 50–300 mg/L	90.09	Freundlich	[100]
Banana bract/H_2SO_4	Zn-Al LDHs/AC composite	2 g/L, 30 °C, 40 min, pH 6, 50–150 mg/L	73.23	Freundlich	[127]
Commercial	Polyaniline/AC composite	10 g/L, 25 °C, 2 h, pH 6, 25–200 mg/L	11.04	Sips	[46]
Pine cone/H_3PO_4	Zero valent iron/AC composite	10 g/L, 25 °C, 250 min, pH 6, 20–320 mg/L	26.40	Langmuir- Freundlich	[101]
Papaya seeds/H_2SO_4	$CoFe_2O_3$/AC composite	2 g/L, 30 °C, 40 min, pH 5.3, 50–150 mg/L	78.981	Freundlich	[105]
Sewage sludge/$ZnCl_2$	Magnetic Mg-Fe/LDHs AC composite	5 mg, 25 °C, 250 min, pH 3, 10–50 mg/L	46.3	Langmuir, Freundlich	[96]
Muskmelon peel/H_2SO_4	$ZnFe_2O_4$/AC composite	2 g/L, 30 °C, 2 h, pH 5.6, 50–150 mg/L	75.587	Freundlich	[97]
Coal/commercial	Fe_2O_3/AC composite	6.5 g/L, 25 °C, 24 h, pH 5.5, 25–200 mg/L	17.42	Langmuir	[98]
Apple branch/CO_2	Mg/Al-LDHs AC composite	0.05 g/L, 25 °C, 6 h, pH 3,0–100 mg/L	156.84	Freundlich	[60]
Orange peel/H_2SO_4	Zn-Fe LDHs/AC composite	2 g/L, 30 °C, 1.5 h, pH 6, 50–150 mg/L	71.18	Freundlich	[95]

functionality and porosity of Zr-CS-SAC composite. $ZrOCl_2{\cdot}8\ H_2O$ interacted with the surface groups of chitosan and also Zr^{4+} ions entered the pores of AC which improved the adsorption sites. Zr^{4+} ions, NH^{3+}, and OH^{2+} also offered the positive surface charge which favored the attraction of nitrate [58].

Section 3 shows that chemical activation is the extensively used technique for production of raw ACs as adsorbents for nitrate. In this regard, $ZnCl_2$ and H_3PO_4 are the most widely applied chemical agents. From the data (Table 1), these agents exhibit maximum surface areas of 1826.0 and 1090.0 m^2/g for ACs derived from sugar beet bagasse and orange peel, respectively. Alkalis, acids, surfactants, magnetic agents, urea, amines, etc. are utilized as modifying agents for raw ACs. Among these, surfactants as well as magnetic and nitrogen-containing compounds represent the most applied and highly efficient agents for this

Table 3
Kinetic study conditions and results of nitrate ions removal using different AC-based adsorbents.

Precursor/activator	Adsorbent	Kinetic conditions	Equilibrium time	Rate constant k_2 g/mg.min	Kinetic	Ref.
Finnish wood chips/CO_2	Raw AC	5 g/L, rT, 1 min-24 h, pH 4, 10 mg/L	24 h	5.619	PSO	[45]
Coconut shells/ Steam	Raw AC	5 g/L, rT, 1 min-24 h, pH 4, 20 mg/L	24 h	0.0537	PSO	[45]
Olive jift/$ZnCl_2$	Raw AC	20 g/L, 20 °C, 0–150 min, pH 4, 200 mg/L	90 min	0.0483	PSO	[118]
Finnish wood chips/$ZnCl_2$	Raw AC	5 g/L, rT, 1 min-24 h, pH 6, 25 mg/L	24 h	0.046	PSO	[55]
Commercial	Raw AC	10 g/L, °C, 0–300 min, pH 2, 100 mg/L	45 min	0.280	PSO	[130]
Sugar beet bagasse/$ZnCl_2$	Raw AC	2 g/L, 45 °C, 25–360 min, pH 6.58, 100 mg/L		0.0011	PSO	[51]
P. juliflora branches/H_2SO_4	Raw AC	1 g/L, 30 °C, 0–300 min, pH 6.7, 50 mg/L	60 min	0.0199	PSO	[52]
Sugar cane bagasse/ H_3PO_4	Raw AC	10 g/L, 25 °C, 10–90 min, pH 4, 25 mg/L	30 min	2.6873	PSO	[119]
Coal/commercial	Raw AC	2 g/L, 25 °C, 0–28 h, pH 5, 200 mg/L	6 h	0.0031	PSO	[124]
Commercial	Raw AC	66.7 g/L, 20 °C, 45–120 min, pH 6.5, 100 mg/L	60 min	0.115	PSO	[120]
Oil palm shells/H_3PO_4-steam	Raw AC	5 g/L, rT, 5–80 min, pH 2, 10 mg/L	70 min	5.433	PSO	[48]
Oil palm shells/KOH-steam	Raw AC	5 g/L, rT, 5–80 min, pH 2, 10 mg/L	70 min	5.014	PSO	[48]
C. carandas stems/H_2SO_4	Raw AC	1.3 g/L, 30 °C, 0–60 min, pH 7, 10 mg/L	50 min	0.019	PSO	[113]
Pomegranate peel/ H_3PO_4 +$ZnCl_2$	Raw AC	5–80 g/L, 20 °C, 0–120 min, pH 7.2, 100 mg/L	45 min	0.0027	PSO	[114]
P. aculeate trunks /K_2CO_3	Raw AC	10 g/L, 25 °C, 0–400 min, pH 2, 1.61 mmol/L	300 min	0.0161	PSO	[57]
P. aculeate trunks /NH_4Cl	Raw AC	10 g/L, 25 °C, 0–400 min, pH 2, 1.61 mmol/L	30 min	0.0726	PSO	[57]
Rice husk/NaOH	Raw AC	2 g/L, 20 °C, 0–3 h, pH, 50–400 mg/L	1 h	0.0072–0.0048	PSO	[49]
Coir pith/$ZnCl_2$	Raw AC	4 g/L, 35 °C, 0–15 min, pH 3, 10–40 mg/L	5 min	3.1969–1.8146	PSO	[50]
Rice straw/Na_2CO_3	Raw AC	2.5 g/L, 25 °C, 0–24 h, pH>7, 50 mg/L	10 h	0.0028	PSO	[53]
Sucrose	Raw AC	0.96 g/L, 21 °C, 0–100 min, pH 7–8, 2 mg/L		0.070	PSO	[121]
Shrimp shell/$ZnCl_2$	Raw AC	2.5 g/L, 25 °C, 0–60 min, pH 3, 20 mg/L	10 min	0.540	PFO	[54]
G. globra residues/$ZnCl_2$	Raw AC	4 g/L, 35 °C, 0–300 min, pH 2, 50 mg/L	90 min	0.020	PSO	[56]
Lignite	Cationic polymer modified AC	2.5 g/L, 23 °C, 0–240 min, pH 6.65, 43.2 mg/L	90 min	0.006	PSO	[88]
Lignite	Raw AC	2.5 g/L, 23 °C, 0–240 min, pH 6.65, 43.2 mg/L	90 min	0.018	PSO	[88]
Banana bract/H_2SO_4	Amine/Fe_3O_4 modified AC	2 g/L, 30 °C, 0–90 min, pH 7, 50–150 mg/L	40 min (100 mg/L)	0.487–0.391	PSO	[82]
Coconut/commercial	$ZnCl_2$ modified AC	10 g/L, 20 °C, 0–12 h, pH n, 10–100 mg/L	60 min	0.0034–0.0009	PSO	[73]
Rice straw/steam	$KMNO_4$ modified AC	2 g/L, rT, 0–24 h, pH, 50 mg/L	10 h	0.0045		[77]
Lignite/commercial	$ZnCl_2$ modified AC	10 g/L, 25 °C, 1–120 min, pH 5, 25–115 mg/L	30–90 min	0.482–0.036	PSO, PFO	[74]
Coconut shell/steam	$ZnCl_2$ modified AC	10 g/L, 25 °C, 5–60 min, pH 5.5, 25, 50 mg/L	60 min	0.0791, 0.0260	PSO	[59]
Commercial	$CaCl_2$ modified AC	20 g/L, 25 °C, 5–120 min, pH 6, 10, 20 mg/L	60, 30 min	25.80, 37.30	PSO	[91]
Date stems/$ZnCl_2$	Surfactant modified AC	1 g/L, 25 °C, 0–30 min, pH 5.6, 100 mg/L	5 min	0.209	PSO	[84]
Grape wood/H_2SO_4	Iron modified AC	6 g/L, 25 °C, 5–60 min, pH 4, 150 mg/L	35 min	0.0047	PSO	[67]
C. manni naudin shells/ $ZnCl_2$	Amine modified AC	1 g/L, 27 °C, 0–90 min, pH 3, 50 mg/L	50 min	0.266	PFO	[71]
Vetiver grass/KOH	ZR/CTAB modified AC	6 g/L, 25 °C, 0–120 min, pH 3, 20–40 mg/L	60 min	0.439–1.028	PSO	[80]
Commercial	CTAC modified AC	2.5 g/L, 25 °C, 0–270 min, pH 7, 20 mg/L	30 min	0.079	PSO	[64]
Commercial	Fe_3O_4 modified AC	1 g/L, 20 °C, 0–180 min, pH 3, 100 mg/L	60 min	0.002	PSO	[85]
Rice straw/steam	$KMNO_4$ modified AC	2.5 g/L, 25 °C, 0–24 h, pH 3–9, 50 mg/L	10 h	0.0045	PSO	[61]
Commercial	Fe^{2+}, H_2O_2 modified AC	1.5 g/L, 25 °C, 0–2 h, pH 4, 10–50 mg/L	1 h	0.005–0.0018	PSO	[81]
Coconut shell	NaOH-CTAB modified AC	4 g/L, 25 °C, 0–9 h, pH 7, 40–80 mg/L	2 h	0.0022–0.0018	PSO	[63]
Corn straw/ H_3PO_4	$FeCl_3$ modified AC Magnetic	0.83 g/L, 25 °C, 0–24 h, pH 6, 30 mg/L	4 h	0.0016	PSO	[65]
Corn straw/ H_3PO_4	Raw AC	0.83 g/L, 25 °C, 0–24 h, pH 6, 30 mg/L	4 h	0.0013	PSO	[65]
Sucrose/H_2SO_4	Amino modified AC	3 g/L, 25 °C, 0–120 min, pH 7, 100 mg/L	5 min	0.0324	PSO	[72]
Strip moso bamboo/H_3PO_4	quaternary nitrogen modified AC	2 g/L, rT, 0–20 min, pH 3, 200 mg/L	8 min	0.0374	PSO	[75]
Apple branch/CO_2	Mg/Al-LDHs AC composite	0.05 g/L, 25 °C, 0–24 h, pH 3, 60 mg/L	6 h	0.010	PSO	[60]
Orange peel/H_2SO_4	Zn-Fe LDHs/AC composite	2 g/L, 30 °C, 0–90 min, pH 6, 50–150 mg/L	30 min (100 mg/L)	0.0914–0.0983	PSO	[95]
Pine cone/H_3PO_4	Zero valent iron/AC composite	10 g/L, 25 °C, 0–24 h, pH 6, 100 mg/L	250 min	0.016	PSO	[101]
Sewage sludge/$ZnCl_2$	Magnetic Mg-Fe/LDHs AC composite	5 mg, 25 °C, 0–360 min, pH 3, 10–50 mg/L	250 min	0.0184–0.0322	PFO	[96]
Coal/commercial	Fe_2O_3/AC composite	6.5 g/L, 25 °C, 10–60 min, pH 5.5, 150 mg/L	60 min	0.0790	PSO	[98]
Muskmelon peel/H_2SO_4	$ZnFe_2O_4$/AC composite	2 g/L, 30 °C, 0–120 min, pH 5.6, 50–150 mg/L	50 min (100 mg/L)	0.489–0.164	PSO, IPD	[97]
Papaya seeds/H_2SO_4	$CoFe_2O_3$/AC composite	2 g/L, 30 °C, 0–120 min, pH 5.3, 50–150 mg/L	40 min (100 mg/L)	0.476–0.387	PSO, IPD	[105]
Coal fine slag	Silica/AC composite	2.5 g/L, 20 °C, 0.5–10 h, pH 6, 20 mg/L	10 h	0.7617	PSO	[102]
Soya bean husk/H_2SO_4	Zr^{4+} embedded chitosan/AC composite	2 g/L, 30 °C, 5–70 min, pH 6.4, 100–200 mg/L	45 min (100 mg/L)	0.022–0.029	PSO	[100]
Banana bract/H_2SO_4	Zn-Al LDHs/AC composite	2 g/L, 30 °C, 0–120 min, pH 6, 50–150 mg/L	40 min	0.111–0.141	PSO, IPD	[127]
Commercial	Polyaniline/AC composite	10 g/L, 25 °C, 0–120 min, pH 6, 25–75 mg/L	30 min	0.187–0.0257	PSO	[46]

PSO: Pseudo-second order, PFO: Pseudo-first order, IPD: Intraparticle diffusion.

purpose. These modifications can improve the adsorption performance mainly by introducing new active groups (for example –CH_2, Fe–O, and –NH_2) and providing the positively charged functionality which favors the attraction of anionic nitrate. Moreover, some of the mentioned modifications such as magnetic can also improve the porosity. Another modification form is composite with materials like layered double hydroxides (LDHs), iron oxides, zeolite, chitosan, etc. The combination with the most widely used materials such as LDHs and iron oxides provide more positively charged binding sites, which effectively enhance the nitrate adsorption. Iron oxides can also develop the porous structure of raw ACs.

4. Adsorbents performance

In general the performance of AC-based adsorbents towards nitrate is indirectly affected by their physical and chemical characteristics such as pore properties, elemental composition, pH, etc. These parameters are dependent on the preparation variables including activation temperature, activation time, and amount and type of activating agent along with the type of activation method. Moreover, the performance directly depends on adsorption variables in terms of inlet adsorbate amount, adsorbent dose, solution pH, and temperature.

4.1. Influence of preparation variables

In adsorption processes, the capacity represents the most essential feature of an adsorbent which is mainly depended on its pore properties. Generally, the higher capacity of AC is related to the larger surface area so it is necessary to explore the variables which influence the activation extent and surface area [45]. Porous structure is improved by the activation methods. Activation temperature and time, impregnation ratio, and activating agent type are the most significant variables for AC preparation.

Activation temperature favorably affects the pore development. In this regrad, Pan et al. [54] tested the influence of activation temperature on pore and nitrate adsorption properties of shrimp shells/$ZnCl_2$ derived AC. At constant impregnation ratio of 1:1 shell/$ZnCl_2$ ratio, the raise in temperature from 400 °C to 600 °C exhibited an increase in BET surface area from 496.9 to 773.5 m^2/g, total pore volume from 0.200 to 0.290 cm^3/g, and average pore radius from 0.630 to 0.750 nm. Elevating the activation temperature enhances the releasing of volatiles from the structure of precursor, causing an enhancement in the development of existing pores and creation of new pores [51,56]. Accordingly the adsorption performance towards nitrate for AC obtained at 600 °C was about 1.4 times more than that obtained at 400 °C. The activation step developed the porosity of the biochar precursor and thus provided more active sits in ACs' structure, which considerably improved the capacity.

However, higher activation temperature can destroy the porous structure of AC, as explained by Zhang et al. [49] who showed the influence of activation temperature on the pore properties of rice husk-AC by NaOH activation. The values of surface area, pore volume, and average pore size were 2526, 2802, 1857 m^2/g, 1.517, 1.690, and 1.389 cm^3/g, and 1.200, 1.210, and 1.500 nm for ACs obtained at 500, 600, and 700 °C. Thus, the increase in surface area followed the order: AC600 > AC500 > AC700. This behavior could be due to the turning of many micropores into mesopores at 700 °C [41]. Consequently, the microporous AC600 had the highest surface area of 2802 m^2/g. The ash contents of ACs were 3.94, 3.52, and 3.23 (wt%) at 500 °C, 600 °C, and 700 °C.

Activation time is an essential variable that identifies the sufficient contact between the precursor and activating agent under other specific activation conditions. Kilpimaa et al. [45] tested the influence of this parameter on the porous structure of AC prepared by the physical CO_2 activation of Finnish wood chips-biochar precursor. During the activation at temperature of 800 °C, the increase in time from 1 to 3 h changed the pore properties from 353 m^2/g, 0.340 cm^3/g, and 3.86 nm into 590 m^2/g, 0.335 cm^3/g, and 3.44 nm, respectively. The enhancement in BET surface area could be related to the increase in burn-off from 40.1 % to 55.2 % when duration of activation increased from 1 to 3 h. According to the results, the activation time had a lower significant role in developing porosity compared to the activation temperature.

Another variable, influencing the pore characteristics, is the ratio of impregnation. It is identified by the amount of the activator divided by the amount of the precursor. This parameter also favorably improves the pore properties of AC. In this regards, Demiral and Gündüzoğlu [51] explored the influence of impregnation ratio on the pore properties of sugar beet bagasse derived AC using of $ZnCl_2$ as chemical agent. At

Table 4
Thermodynamic study conditions and results of nitrate ions removal using different AC-based adsorbents.

Precursor/activator	Adsorbent	Thermodynamic conditions	ΔH (kJ/mol)	ΔS (J/mol.K)	ΔG (kJ/mol)	Ref.
Olive jift/$ZnCl_2$	Raw AC	20 g/L, 10–40 °C, 24 h, pH 4, 100–300 mg/L	-13.859	-43.795	-1.217 to − 0.028	[118]
Commercial	Raw AC	20 g/L, 10–40 °C, 24 h, pH 4, 100–300 mg/L	-15.099	-62.518	2.798–4.582	[118]
Sugar beet bagasse/$ZnCl_2$	Raw AC	2 g/L, 25–45 °C, 6 h, pH 6.58, 10–200 mg/L	133.62	0.516	-20.75 to − 31.15	[51]
P. juliflora branches/H_2SO_4	Raw AC	1 g/L, 20–40 °C, 1 h, pH 6.7, 1–100 mg/L	30.94	0.090	-3.26 to − 1.52	[52]
Sugar cane bagasse/ H_3PO_4	Raw AC	10 g/L, 25–55 °C, 0.5 h, pH 4, 5–40 mg/L	7.486	-3.242	0.973–1.071	[119]
Coir pith/$ZnCl_2$	Raw AC	4 g/L, 35–60 °C, 20 min, pH 3, 10–40 mg/L	27.54	100.82	-3.197 to − 5.846	[50]
Rice straw/Na_2CO_3	Raw AC	4 g/L, 25–55 °C, 24 h, pH>7, 0–25 mg/L	-12.8	-0.76	2.80–4.40	[53]
C. carandas stems/H_2SO_4	Raw AC	1.3 g/L, 30–50 °C, 50 min, pH 7, 10–150 mg/L	16.1	97.27	− 13.37 to − 15.32	[113]
G. globra residues/$ZnCl_2$	Raw AC	4 g/L, 25–45 °C, 90 min, pH 2, 20–100 mg/L	15.555	114.36	-18.3 to − 20.8	[56]
Coconut shell	NaOH-CTAB modified AC	4 g/L, 25–45 °C, 2 h, pH 7, 40–200 mg/L	-56.68	-132.0	-17.10 to − 14.44	[63]
Sucrose/H_2SO4	Amino modified AC	3 g/L, 25–45 °C, 1 h, pH 7, 50–250 mg/L	-73.223	-245.589	-0.037–4.874	[72]
Lignite	Cationic polymer modified AC	2.5 g/L, 25–45 °C, 4 h, pH 6.65, 25–376 mg/L	-21.45	30.32–100.2	-30.48 to − 31.88	[88]
Banana bract/H_2SO_4	Amine/Fe_3O_4 modified AC	2 g/L, 30–50 °C, 1.5 h, pH 7, 50–150 mg/L	6.54	16.50	-6.81 to − 7.89	[82]
Lignite/commercial	$ZnCl_2$ modified AC	10 g/L, 10–45 °C, 24 h, pH 5, 5–150 mg/L	6.13	26.95	-1.546 to − 2.490	[74]
Coconut shell/steam	$ZnCl_2$ modified AC	10 g/L, 10–45 °C, 2 h, pH 5.5, 5–200 mg/L	-13.16	-33.0	-4.01 to − 2.75	[59]
Vetiver grass/KOH	ZR/CTAB modified AC	6 g/L, 25–45 °C, 120 min, pH 3, 20–40 mg/L	6.201	0.011	-9.226 to − 9.409	[80]
Commercial	Fe_3O_4 modified AC	1 g/L, 20–45 °C, 60 min, pH 3, 50–300 mg/L	88.5	0.370	-2.98 to − 3.92	[85]
Rice straw/steam	$KMNO_4$ modified AC	4 g/L, 25–55 °C, 24 h, pH 3–9, 50 mg/L	-12.8	-0.76	2.80–4.40	[61]
Muskmelon peel/H_2SO_4	$ZnFe_2O_4$/AC composite	2 g/L, 30–50 °C, 2 h, pH 5.6, 50–150 mg/L	6.76	16.5	-6.91 to − 7.88	[97]
Soya bean husk/H_2SO_4	Zr^{4+} embedded chitosan/AC composite	2 g/L, 30–50 °C, 45 min, pH 7, 50–300 mg/L	52.36	0.18	-11.14 to − 9.31	[100]
Banana bract/H_2SO_4	Zn-Al LDHs/AC composite	2 g/L, 30–50 °C, 40 min, pH 6, 50–150 mg/L	21.70	10.10	-6.76 to − 6.91	[127]
Commercial	Polyaniline/AC composite	10 g/L, 25–45 °C, 2 h, pH 6, 25–200 mg/L	-11.84	55.52	-28.34 to − 29.47	[46]
Orange peel/H_2SO_4	Zn-Fe LDHs/AC composite	2 g/L, 30–50 °C, 1.5 h, pH 6, 50–150 mg/L	27.80	0.010	-8.90 to − 9.03	[95]
Papaya seeds/H_2SO_4	$CoFe_2O_3$/AC composite	2 g/L, 30–50 °C, 40 min, pH 5.3, 50–150 mg/L	8.67	16.91	-7.56 to − 7.89	[105]
Sewage sludge/$ZnCl_2$	Magnetic Mg-Fe/LDHs AC composite	5 mg, 25–45 °C, 250 min, pH 3, 10–50 mg/L	4.90	28.5	-3.64 to − 4.21	[96]

constant temperature of 700 °C, the increase in $ZnCl_2$/bagasse ratio from 1 to 3 caused an increase in S_{BET} from 1389 to 1826 m^2/g, V_T from 0.650 to 0.966 cm^3/g, and d_P from 1.87 to 2.22 nm. However, V_{micro} increased from 0.498 to 0.760 cm^3/g with the change of impregnation ratio from 1 to 2, and then decreased to 0.711 cm^3/g at ratio 3. The large quantity of $ZnCl_2$ reduces the formation of tar formation and enhances the liberation of volatiles, thereby pore properties improved [106,107]. However, micropore volume increases with increasing impregnation ratio up to 2 and then it exhibits a pronounced decrease at ratio of 3. These observations indicated that as the ratio of impregnation is larger than 2, the high impeding in the formation of tar by the $ZnCl_2$ caused the liberation of more volatiles from the structure of carbon. This led to a significant rise in pore enlargement. Numerous micropores were turned to mesopores. Accordingly, the surface area and micropore volume declined. The phenomenon of pore enlargement was also observed in the literature [108]. As the $ZnCl_2$/bagasse ratio increased from 2 to 3, the micropore volume reduced from 85.15 % to 73.60 %. It was proposed that the $ZnCl_2$ activator formed new pores and also enlarged existing pores, so that a considerable number of micropores turned into mesopores. The average pore width enhanced from 1.87 to 2.22 nm with the ratio changing from 1 to 3. The influence of impregnation ratio on surface area was relatively less significant compared to the activation temperature.

The increase of impregnation ratio can enhance the adsorption performance of AC towards nitrate, as explained by Najmi et al. [56] who studied the effect of impregnation ratio for nitrate removal by *Glycyrrhiza glabra* residues derived AC through chemical activation using $ZnCl_2$. At constant activation temperature of 850 °C, the increase in $ZnCl_2$/residues ratio from 1:1–2:1, enhanced nitrate removal efficiency from 65.78 % to 79.12 %. The $ZnCl_2$ develops microporosity and positively charged surface functionality of AC structure; thus, the removal of nitrate would enhance by enlarging the $ZnCl_2$/residues ratio [59].

The effect of activating agents on pore properties and performance of ACs was also included in the literature. Zhang et al. [49] prepared rice husk-AC with a high surface area of 2802 m^2/g by NaOH activation. This value was higher than those reported for rice husk derived ACs by $ZnCl_2$ 811 m^2/g [109] and H_3PO_4 451.82 m^2/g [110]. The ash contents of NaOH AC and $ZnCl_2$ AC were 3.52 % and 27.8 %, respectively. NaOH AC showed a lower ash content relative to $ZnCl_2$ AC due to the tendency of NaOH to react with SiO_2 [43]. The results confirmed that NaOH activation was an efficient way for producing ACs with large surface area small ash content. The amounts of ash in ACs were lower than the large amount of 12.5 % in rice husk. NaOH was reacted with SiO_2 during the activation process which resulted in opening of blocked pores and reducing of ash content [111]. This suggested that NaOH could efficiently eliminate ash and enhance the porous structure of carbon. The morphology indicated that the carbon exhibited a developed structure with some mesopores and macropores heterogeneously spread on the surface.

Another team [55] tested the chemical activation of Finnish wood chips-biochar to produce AC. Different activating agents were utilized such as HCl (0.1 M), H_2SO_4 (0.1 M), HNO_3 (65 %), $ZnCl_2$ (5 M), and KOH (5 M). The highest surface area of 285 m^2/g was reported by $ZnCl_2$ (5 M) relative to 14.4 m^2/g for carbon residue. During the activation step, carbon residue was treated with 5 M $ZnCl_2$ solution at an impregnation ratio of 10:1 for 1 h. Cavities are created because of the $ZnCl_2$ evaporation which demonstrates the enhancement in surface area [112]. The C content was 63.8 % for carbon residue and 61.8 % for AC, the H content was 1.7 % for carbon residue and 0.75 % for AC, the specific surface area was 14.4 m^2/g for carbon residue and 285 m^2/g for AC, the average pore size was 8.38 and 3.94 nm, and the total pore volume was 0.03 and 0.26 cm^3/g. The performance in terms of removal % for activated carbon was about three times (3.0) more than that of carbon residue (precursor). In terms of q_{exp} it is about 2.82 times that of carbon residue.

Nunell et al. [70] explored the influences of H_3PO_4 and KOH on the physico-chemical characteristics of *P. aculeata* wood sawdust –AC. The textural properties of ACA were S_{BET} of 968 m^2/g, V_t of 0.70 cm^3/g, V_{micro} of 0.18 cm^3/g, and d_p of 2.9 nm compared to 768 m^2/g, 0.37 cm^3/g, 0.27 cm^3/g, and 1.9 nm for ACB. Textural parameters indicated that H_3PO_4 activation produced AC of largest total pore volume and BET surface area relative to those reported for KOH. ACB exhibited the largest micropores volume; meanwhile the enrichment of mesopores recognized the ACA structure. The amounts of basic and acidic surface groups were 0.1 and 1.9 mmol/g for ACA and 0.7 and 1.2 mmol/g for ACB. ACA had larger amount of acidic groups relative to the ACB. Moreover, only the ACB activated with KOH showed a significant content of basic groups (0.7 mmol g1). In contrary, the ACA exhibited a small amount of basic groups (0.1 mmol/g). ACs with basic functionality can efficiently attract anionic specie, at low pH [71]. For H_3PO_4 AC the removal % and uptake were 30 % and 0.045 mmol/g. For KOH AC the removal% and uptake were 62.5 % and 0.10 mmol/g. From the Langmuir model, the magnitudes of q_{max} were 0.30 and 0.11 mmol/g for base and acid AC.

Kilpimaa et al. [45] adopted the physical activation technique to prepare AC from Finnish wood chips-biochar precursor. The influence of activation time on the characteristics of AC was tested. Physical activation was performed by adopting two different activators in terms of CO and CO_2. For CO_2 and CO activations, the maximum BET surface area, pore volume, and average pore width were 590 m^2/g, 0.335 cm^3/g, and 3.44 nm; and 133 m^2/g, 0.205 cm^3/g, and 6.16 nm at the conditions of 800 °C and 3 h. This result could be related to the high burn-off of 55.2 % in the case of CO_2 activation as compared to 25.6 % for CO.

For modified AC-based adsorbents, the effect of modifying agent amount on the performance for removal of nitrate was considered by researchers. For instance, Cho et al. [88] tested the influence of cationic polymer amount on nitrate removal by polymer modified AC (from lignite precursor). BET surface area of raw AC was reported as 1159 m^2/g. Polymer modification caused a decline in surface area, giving 1003, 945 and 492 m^2/g as the amount of polymer changed to 0.025 %, 0.25 % and 2.5 %, respectively. This behavior indicated that the polymer had blocked the pores and inhibited the access of adsorbate [81]. The nitrate uptake of AC enhanced from 4.71 to 9.16 mg/g as the amount of polymer enlarged from 0 % to 0.25 %, and removal performance enhanced approximately twice (43.75–86.25 %). It was suggested that the existence of quaternary ammonium surface groups played a key role in the enhancement of nitrate removal and the amount of surface groups on AC mainly depended on the ratio of AC to polymer. At 2.5 % polymer, the nitrate uptake of AC declined insignificantly to 7.52 mg/g relative to 0.25 % (removal declined to 70.83 %). The decrease in removal performance could be due the hiding of active sites in AC pores by surplus polymer which consequently declined surface area available for adsorption. Also, the values of adsorption capacity for nitrate by Langmuir model (14.25 and 27.56 mg/g, respectively) use raw and modified ACs.

4.2. Influence of adsorption variables

The most significant variables that influence adsorption performance are inlet adsorbate amount, adsorbent dose, temperature, and solution pH. Each of these factors has a specified effect on the adsorption behavior of nitrate on AC-based adsorbents.

Initial amount of nitrate and dosage of AC-based adsorbents exhibit a constant and different influence on the adsorption efficiency. The influence of these parameters mainly depends on the relation between the amount of nitrate in the solution and the number of active sites on the AC-based adsorbents surface. In general, increasing the inlet nitrate amount can improve the adsorbed amount of nitrate. However, this increase causes a decline in removal percentage. For instance, Manjunath and Kumar [52] showed that increasing the inlet NO_3^- amount from 1 mg/L to 100 mg/L exhibited an enhancement in capacity q_e of

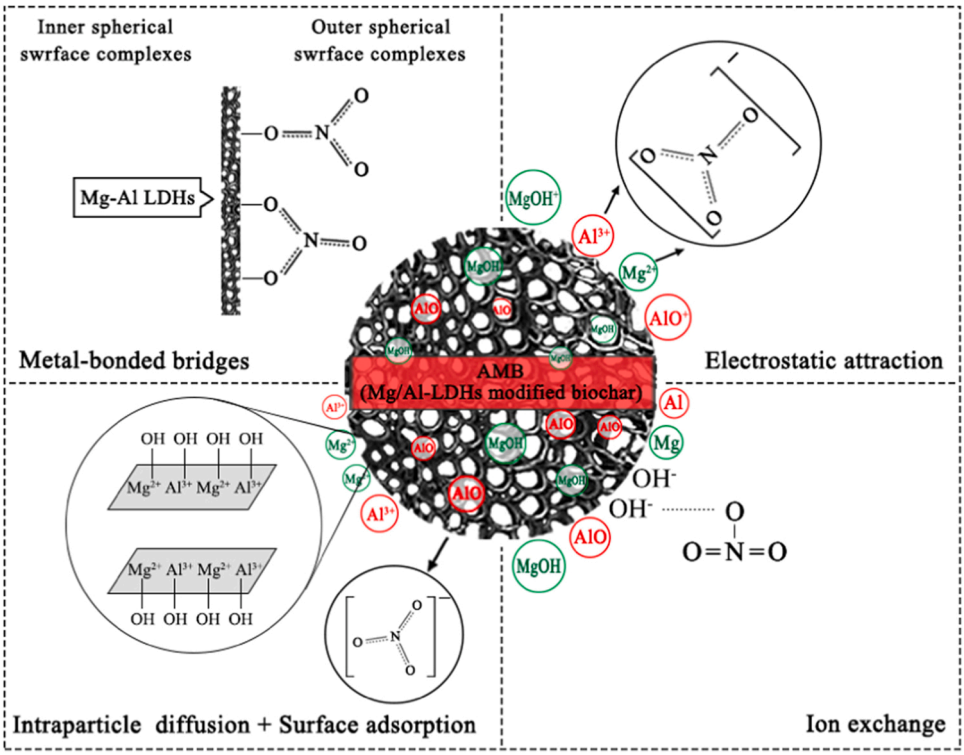

Fig. 5. Schematic illustration of the possible adsorption mechanisms for nitrate by Mg/Al-LDHs apple branch/CO_2 AC composite [60].

Prosopis juliflora branches derived AC adsorbent towards NO_3^- from 0.90 mg/g to 23.58 mg/g and a decrease in removal percentage from 89.9 % to 23.6 %, respectively. This might be attributed to higher concentration gradient between the solution bulk and the adsorbent surface which caused the diffusion of more NO_3^- ions towards the active sites of adsorbent and thereby leading to higher adsorptivity. On the other hand, the decline in removal was due to the little number of available active sites relative to the amount of NO_3^- ions [80,85,113]. The increase in adsorbent dosage exhibits an opposite effect on the adsorption performance as compared to initial NO_3^- concentration. In this regard, Mazarji et al. [63] reported that as the dosage of NaOH-CTAB modified AC raised from 1 to 10 g/L, the uptake reduced from 11 to 3.3 mg/g, whereas the removal of nitrate enhanced from 25 % to 83 %. This could be due to the decrease of the driving force with the enlargement of the adsorbent/adsorbate ratio [61,64]. However, the increased removal percentage might be attributed to the existence of more adsorption sites with increasing of adsorbent dose at constant NO_3^- concentration and volume [81].

Solution pH is another parameter that affects the removal performance of AC-based adsorbents for NO_3^- ions by changing the electrostatic interaction type between the adsorbents and NO_3^- ions. In the literature, two behaviors have been reported for the influence of solution pH on the removal performance of studied systems. The first one is the decrease of NO_3^- uptake with raising the pH value. For example, Pan et al. [54] showed that the adsorbed amount of nitrate on shrimp shells/$ZnCl_2$ derived AC decreased from 5.58 to 4.43 mg/g with increasing the pH value from 3.0 to 10.0. With the increase of pH from 3.0 to 10.15, the nitrate removal on sugar beet bagasse/$ZnCl_2$ derived AC declined from 41.2 % to 34.68 %. Highest adsorption (41.2 %) was reported at pH 3 [51]. This behavior could be due to the high protonation of functional groups at lower pH, thereby the adsorbent surface had more positive charges, which enhanced the attraction forces toward the NO_3^- anions. Thus, more acidic solution favors the adsorption of NO_3^- ions [70,71,108]. The second behavior is the increase of adsorption performance with increasing of solution pH to a specific value, and then decreases. For instance, Karthikeyan et al. [105] showed that the adsorption capacity of $CoFe_2O_3$/AC composite for NO_3^- increased with changing pH from 2 to 7, and then declined at pH higher than 7. The maximum adsorbed amount was about≈ 38 mg/g at pH 7. The value of pH for adsorbent at the point of zero charge (pH_{PZC}) was 6.9. The surface has positive charges at $pH<pH_{PZC}$ and negative charges at $pH>pH_{PZC}$. Nitrate removal was favorable at $pH<pH_{PZC}$. However, smaller removal at highly acidic solution (pH 2) was due to the fact that Cl^- ions (from HCl used to modify the pH) competed with nitrate ions towards the active sites. Also, lower NO_3^- removal at $pH>pH_{PZC}$ was due to existence of more competing OH^- ions which caused a strong repulsion for NO_3^- ions from the surface of adsorbent [67,74,114,115].

Temperature is an essential adsorption variable that substantively affects the NO_3^- uptake of AC-based adsorbents. The influence of temperature shows an inconsistent behavior for NO_3^- removal, which relates to the exothermic/endothermic adsorption nature of the studied system. The endothermic behavior in terms of high adsorption capacity for NO_3^- at high temperatures is reported in most of the studies. In this regard, Demiral and Gündüzoğlu [51] showed that the adsorption capacity sugar beet bagasse/$ZnCl_2$ derived AC for NO_3^- enhanced from 9.14 to 27.55 mg/g with increase in temperature from 25 °C to 45 °C, respectively. The increase in uptake might be due to surface activation, enlargement of pores on adsorbent, rising in NO_3^- mobility along with decreased swelling nature of AC [52,113]. On the other hand, the exothermic behavior for NO_3^- adsorption is also observed in the literature. For instance, Cho et al. [88] showed a decline in the uptake of cationic polymer treated AC for NO_3^- from 29.4 to 24.4 mg/g with raising temperature from 25 °C to 45 °C. This was related to the solubility of the nitrate. The value of KNO_3 solubility enhanced from 0.316 g/mL water at 20 °C to 1.10 g/mL water at 60 °C [53]. Another possible reason could be due to the lowering of pH_{PZC} value of adsorbent which resulted in a more negatively charged surface. This behavior reduced the removal of anions [61].

The significance of adsorption parameters on the performance of AC-based adsorbents for nitrate ions was identified by using response surface methodology RSM and analysis of variance ANOVA. In this regard, Taoufik et al. [116] showed that the influence of both initial nitrate

concentration and AC dosage were more significant on the removal performance of a commercial raw AC as compared to solution pH. Similar observations were recorded by Mehrabi et al. [98] for nitrate adsorption on Fe_2O_3/AC composite. Najmi et al. [56] showed that the initial nitrate concentration had the largest effect on the elimination of nitrate by *Glycyrrhiza glabra* residues/$ZnCl_2$ derived AC, followed by solution pH and temperature. Hu et al. [46] also reported that both adsorbent dosage and initial nitrate concentration significantly affected nitrate uptake relative to temperature for adsorption on polyaniline/AC composite.

5. Adsorption isotherms

Adsorption isotherm is an equilibrium relationship that links the remaining and adsorbed amount of an adsorbate toward an adsorbent at fixed conditions [117]. The parameters resulted from modeling of experimental equilibrium data give significant information for the appropriate analysis and design of adsorption unit [37]. The most applied models for the correlation of adsorption isotherm data of nitrate on AC-based adsorbents in terms of Langmuir, Freundlich, Temkin, Dubinin-Radushkevich, Langmuir-Freundlich or Sips, Redlich-Peterson, and Elovich are summarized in Table S1 (Supplementary data). The maximum adsorption capacities of AC-based adsorbents towards nitrate under specified adsorption conditions along with the best applied isotherm models are presented in Table 2. This table indicates that the majority of studies on nitrate adsorption are best analyzed by the Langmuir isotherm model, followed by the Freundlich adsorption isotherm model [118–127].

In this context, Manjunath and Kumar [52] observed that the equilibrium data of nitrate adsorption on *Prosopis juliflora* branches/ H_2SO_4 AC were well-fitted with Langmuir model with the highest R^2 of 0.991 and the lowest average relative error *ARE* of 4.337 compared to other isotherms like Freundlich, Temkin, D-R, and Elovich. This indicated a monolayer adsorption of NO_3^- onto uniform adsorbent sites [118]. Moreover, the values of equilibrium or separation parameter (R_L) were within the range $0 < R_L < 1$ which indicated the favorability of the process [63]. Another team [100] showed that the best convenient model for nitrate adsorption on Zr^{4+} ions modified chitosan-soya bean husk AC composite was Freundlich with the higher R^2 values (0.995–0.998) and lower χ^2 values (0.025–0.121) than Langmuir and D-R isotherms. This reflected the multilayer adsorption behavior on heterogeneous surfaces [60]. The values of $1/n$ (0.654–0.829) lying between 0 and l indicated the favorable adsorption condition [121].

In some cases both the Freundlich and Langmuir models were successfully used for the correlation of NO_3^- equilibrium data on $ZnCl_2$ modified AC [73,74], surfactant modified AC [84], magnetic Mg-Fe/LDHs AC composite [96], and shrimp shell/$ZnCl_2$ derived AC [54]. The Redlich-Peterson model was also good for the adsorption of nitrate on rice husk/NaOH derived AC [49] and on $CaCl_2$ modified AC [91]. Moreover, the Langmuir-Freundlich or Sips model, the two-site Langmuir model exhibited a superior fit than the other models for the systems of NO_3^- on polyaniline/AC composite [46], rice straw/ Na_2CO_3 derived AC [53], zero valent iron/AC composite [101], and $KMNO_4$ modified AC [61]. The models of Redlich-Peterson and Sips merge the characteristics of Freundlich and Langmuir models. They match the Freundlich and Langmuir models at high and low adsorbate amount, respectively [63].

From the data (Table 2), AC-based adsorbents show high performance for nitrate. For example, the highest nitrate uptake of raw AC obtained by the most widely used $ZnCl_2$ activation is 142.58 mg/g. NaOH activation also exhibit raw AC with a high nitrate uptake of 86.20 mg/g. For modified ACs, the highest nitrate uptakes of the most widely tested adsorbents in terms of amine, surfactant, and magnetic modified ACs are 192.92, 83.00, and 58.47 mg/g, respectively. Moreover, AC composites are also efficient adsorbents with high nitrate uptakes of 156.84 mg/g on Mg/Al-LDHs/AC composite and 78.981 mg/g on $CoFe_2O_3$/AC composite.

6. Adsorption kinetics

The kinetic data in terms of adsorbed amount versus time is useful to determine the equilibrium time and rate of an adsorbate/adsorbent system [128]. The parameters resulted from kinetics study are necessary for the correlation of adsorption rate, which provides significant information for modeling and designing the adsorption units, in order to identify both the mechanism and the rate-controlling steps [129].

Table 5
Regeneration study conditions and results of different AC-based adsorbents used for nitrate ions removal.

Precursor/activator	Adsorbent	Eluent	Adsorption; desorption conditions	No. of cycles	Drop in capacity or removal %	Ref.
G. globra residues/ $ZnCl_2$	Raw AC	NaOH	4 g/L, 25 °C, 90 min, pH 2, 50 mg/L; 0.1 M NaOH, 100 mL, 90 min	5	78.0–62.0 %	[56]
C. carandas stems/ H_2SO_4	Raw AC	NaOH	1.3 g/L, 30 °C, 50 min, pH 7, 10 mg/L; 0.1 M NaOH	6	83.5–80.4 %	[113]
Commercial	Fe_3O_4 modified AC	HCl	1 g/L, 25 °C, 60 min, pH 3, 50 mg/L; 0.1 M HCl, 4 h, 30 °C	10	96.1–87.5 %	[85]
C. manni naudin shells/ $ZnCl_2$	Amine modified AC	NaOH	1 g/L, 27 °C, 50 min, pH 3, 200 mg/L; 0.1 M NaOH, 50 min	4	53.33–28.64 mg/g	[71]
Lignite	Cationic polymer modified AC	NaOH	2.5 g/L, 23 °C, 4 h, pH 6.65, 300 mg/L; 0.05 M NaOH, 24 h, 2.5 g/L	4	21.4–14.9 mg/g 81.1–71.4 %	[88]
Banana bract/H_2SO_4	Amine/Fe_3O_4 modified AC	NaOH	2 g/L, 30 °C, 1.5 h, pH 7, 100 mg/L; 0.1 M NaOH, rT, 100 mg	7	71.8–60.0 %	[82]
Soya bean husk/H_2SO_4	Zr^{4+} embedded chitosan/AC composite	NaCl	2 g/L, 30 °C, 45 min, pH 7, 100 mg/L; 0.1 M NaCl, 0.1 g, 60 min	5	38.0–20.7 mg/g	[100]
Banana bract/H_2SO_4	Zn-Al LDHs/AC composite	NaOH	2 g/L, 30 °C, 40 min, pH 6, 100 mg/L; 0.1 M NaOH	5 7	35.0–32.1 mg/g 32.1–25.4 mg/g	[127]
Commercial	Polyaniline/AC composite	NaOH+HCl	10 g/L, 25 °C, 2 h, pH 6, 50 mg/L; 0.1 M NaOH, HCl	1	91.2–87.5 %	[46]
Orange peel/H_2SO_4	Zn-Fe LDHs/AC composite	NaOH	2 g/L, 30 °C, 1.5 h, pH 6, 100 mg/L; 0.1 M NaOH, 40 min, 2 g/L	5 7	85.5–83.5 % 85.5–60.0 %	[95]
Muskmelon peel/ H_2SO_4	$ZnFe_2O_4$/AC composite	NaOH	2 g/L, 30 °C, 2 h, pH 5.6, 100 mg/L; 0.1 M NaOH, 100 mg	7	78.0–58.4 %	[97]
Papaya seeds/H_2SO_4	$CoFe_2O_3$/AC composite	NaOH	2 g/L, 30 °C, 40 min, pH 5.3, 100 mg/L; 0.1 M NaOH, 50 mL	7	78.4–67.5 %	[105]
Sewage sludge/$ZnCl_2$	Magnetic Mg-Fe/LDHs AC composite	NaOH	0.33 g/L, 25 °C, 24 h, pH 3, 10 mg/L; 0.1 M, 0.5 M NaOH	5	74.5–40.0 % 75.5–56.2 %	[96]

Several equations have been applied to analyze the adsorption kinetics of nitrate on AC-based adsorbents, namely pseudo-first order (PFO), pseudo-second order (PSO), intra-particle diffusion (INP), particle diffusion, film diffusion, Elovich, and Bangham models, as summarized in Table S1 (Supplementary data). The equilibrium time and the best applied kinetic model along with its rate constant for studied nitrate/AC-based adsorbents system under specific kinetic conditions are summarized in Table 3.

PSO was best fit in most of the studies. According to Tan et al. [65], the PSO model gave the best fitting for the adsorption kinetics of NO_3^- on magnetic corn straw –AC with R^2 of 0.939 compared to 0.729 for PFO. The result indicated that chemisorption could be the rate-limiting step [63]. The equilibrium state was attained in about 4 h and the rate constant was 0.095 g/mg.h. Zhang et al. [49] observed that the uptake of NO_3^- ions on rice husk derived AC enhanced quickly within the first 30 min and remained approximately fixed beyond 1 h. Furthermore, the magnitudes of q_e and R^2 resulted from the PFO equation were not suitable to represent the adsorption kinetics for NO_3^-. Meanwhile, the computed magnitudes of q_e from the PSO equation agreed with measured data. Moreover, the R^2 were from 0.99 to 1 for the PSO equation. Thus, the kinetics data were best described by the PSO equation. This indicated that the rate of NO_3^- adsorption on AC depended on the available number of active sites rather than the NO_3^- amount in liquid. The PSO rate constant k_2 decreased from 0.43 to 0.29 g/mg.h with increasing the inlet nitrate amount from 50 to 400 mg/L, suggesting that nitrate removal might be more preferable at small adsorbate amount [63]. Accordingly, the adsorbent had a fast adsorption rate at low initial nitrate amounts and could reach equilibrium faster [96]. This behavior could be due strong competition of adsorbate molecules for occupying the active sites at large nitrate amount which enhanced adsorption [81].

PFO model was also applicable to represent the adsorption kinetics of NO_3^- on AC-based adsorbents in terms of $ZnCl_2$ modified lignite-AC [74], ethylenediamine modified Naudin seed shells/$ZnCl_2$ AC [71], magnetic Mg-Fe/LDHs AC composite [96], and shrimp shell/$ZnCl_2$ AC [54]. Moreover, both IPD and PSO were also well applied to identify the mechanism on Zn–Al LDHs/AC composite [127], $ZnFe_2O_4$/AC composite [97], and $CoFe_2O_4$/AC composite [105]. PFO model suggested the physisorption process [71]. IPD identified the rate controlling step in terms of pore diffusion [121].

In general, the effect of contact time on the efficiency of AC-based adsorbents for nitrate removal followed the same behavior. A rapid adsorption at the initial state followed by a slower adsorption and constant or equilibrium states. The existence of many adsorption sites on the ACs surface caused a fast removal of nitrate at the initial state. With the prolongation of time, the saturation or occupying of active sites by adsorbed nitrate and the decline in driving force resulted in a slower adsorption rate. Finally, the equilibrium time was achieved. The equilibrium time was within the range 5 min to 24 h depending on the initial NO_3^- concentration.

7. Adsorption thermodynamics

The thermodynamic analysis provides important information about the nitrate removal. Evaluating the magnitudes of Gibbs free energy, enthalpy, and entropy of adsorption in terms of ΔG°, ΔH°, and ΔS° is useful to identify the type and spontaneity of adsorption system [59,63,72,82].

The most widely used equations that relate the parameters of adsorption thermodynamics in terms of Gibbs and Vant Hoff equations are presented in Table S1 (Supplementary data). The magnitudes of ΔG°, ΔH° and ΔS° for nitrate adsorption on different AC-based adsorbents under identified adsorption conditions are summarized in Table 4. The majority of studies reported negative magnitudes of ΔG° and positive magnitudes for both ΔS° and ΔH° of nitrate removal by AC-based adsorbents. For instance, Demiral and Gündüzoğlu [51] reported ΔH° and ΔS° of 133.62 kJ/mol and 0.516 kJ/mol.K for nitrate adsorption on sugar beet bagasse derived AC. Moreover, the values of ΔG° were − 31.15, − 24.18, and − 20.75 kJ/mol at 45 °C, 35 °C, and 25 °C, respectively. Karthikeyan et al. [82] showed that the magnitudes of ΔS° and ΔH° were 16.50 kJ/mol and 6.54 J/mol.K for nitrate adsorption on amine cross-linked magnetic AC and the values of ΔG° were − 6.81, − 7.45, and − 7.89 kJ/mol at 30 °C, 40 °C, and 50 °C, respectively.

The negative value of ΔG° confirmed that the removal of nitrate by ACs adsorbents was spontaneous. Furthermore, there is a considerable decline in the negativity of ΔG° -value with rising of temperature. This behavior suggested a favorable NO_3^- removal at larger temperatures [85,96], since NO_3^- ions mobility in the liquid along with its affinity for adsorbent, is larger at high temperatures. The positive magnitudes of ΔH° and ΔS° revealed the endothermic process and increasing randomness at the solid-solution interface of the adsorption process, respectively [56,105].

In few studies, the values of ΔG° were positive revealing the non-spontaneous adsorption process [119], revealing the formation of thermodynamically unstable adsorbed species [53,61]. The negative magnitudes of ΔH° and ΔS° were also reported in some studies. This indicated the exothermic nature and the decline in randomness degree at the liquid–solid interface [72].

8. Fixed bed adsorption

Adsorption can be performed in batch and continuous operating modes. The first mode performs in a closed unit; meanwhile the other performs in an open unit in terms of a fixed-bed column [131]. Compared to batch process, fixed bed adsorption columns can treat high volumes of polluted sample and exhibits large adsorption performance. Furthermore, it can be simply turned from a bench to a pilot scale [132]. Basic kinetic data in terms of breakthrough curves are necessary in optimizing and designing continuous adsorption units [133]. In continuous process, the breakthrough curve of a given adsorbate is the plot of the outlet-to-inlet amount (C/C_o) ratio versus time (t). This plot describes the dynamics of a fixed bed unit. The style of the breakthrough curve is affected by different parameters like inlet adsorbate amounts, flow rates, and bed length. The analysis of experimental breakthrough data is important for determining the design parameters and finding the best experimental variables in continuous system [134]. The most extensively applied equations for correlating breakthrough curve data of continuous process are Adams–Bohart and Thomas along with Yoon–Nelson.

Several studies have included the fixed bed removal of nitrate on AC-based adsorbents. In this regard, Manjunath & Kumar [135] tested the continuous adsorption of NO_3^- on *Prosopis juliflora* branches/H_2SO_4 AC. The breakthrough curves were reported at various bed depths, flow rates, and adsorbate amounts. The change in bed height from 5 to 15 cm enhanced breakthrough time from 10 to 50 min. A high breakthrough time was resulted at the large bed depth due to the fact that the lower bed height offered fast saturation relative to the larger bed height. In contrary, the change in flow rate from 0.5 to 2 L/h and influent amount from 25 to 100 mg/L decreased breakthrough time from 80 to 10 min and 30–10 min, respectively. Fast breakthrough was obtained at large flow rates and high inlet NO_3^- concentration due to insufficient contact with the adsorbent and the efficient filling of the adsorbent sites, respectively [136]. Thomas, Yoon-Nelson, Adams and Bohart, as well as bed depth service time models were used to analyze the experimental breakthrough data. The first model exhibited well fitting for the data with a larger determination coefficient ($R^2 > 0.9$) as compared to other models. For Thomas model, computed rate constant, i.e. K_{TH}; was reduced from 7.56 to 3.84×10^4 mL/mg.min and from 4.56 to 3.41×10^4 mL/mg.min with a rise in sorbent depth from 5 to 15 cm and nitrate amount from 25 to 100 mg/L, respectively. While, it was increased from 2.82 to 8.34×10^4 mL/mg.min with rise in flow rate from 0.5 to 2 L/h. This could be due the fact that larger bed height and

larger nitrate amount slows down the rate of mass transfer by increasing the contact time between the AC and adsorbate [20]. On the other hand, large flow rate enhanced the adsorbate mobility, which enhanced the mass transfer and consequently, the K_{TH} magnitude had enhanced with increasing of flow rate.

Fixed bed adsorption of nitrate on raw AC was also considered by Najmi et al. [56] using *Glycyrrhiza glabra* residues (GGR)/$ZnCl_2$ AC as adsorbent. The influence of influent amount and flow rate on the breakthrough curve behavior was tested. According to the result at constant adsorbent height of 10 cm, by changing the nitrate (50 mg/L) flow rate from 10 to 40 mL/min the breakthrough time declined from 76 to 41 min, respectively. At large flow rate, the adsorbate had no enough time to be diffused within the pores of the AC, and thus nitrate exited the column before achieving saturation, leading to bad utilization of the fixed bed [137]. The influence of the inlet nitrate amount of 20, 60, and 100 mg/L at 40 mL/min flow rate and 10 cm bed depth was investigated. From the data, as the initial concentration enhanced, the breakthrough curve tended to be sharper. The time of breakthrough declined from 70 to 20 min, as the initial nitrate amount enlarged from 20 to 100 mg/L. This could be due the fast saturation of the adsorption sites [138]. The breakthrough data were analyzed by Thomas, Yoon–Nelson, and Adams–Bohart models. The first two models were convenient for designing the continuous adsorption unit. All the values of R^2 were higher than 0.94, indicating a best fitting extent. The values of K_{Th} decrease (0.0046–0.0009 mL/mg.min) and the values of q_o increase (58, 811–64,418 mg/g) with changing the initial amount of nitrate (20–100 mg/L). This might be due to the existence of high mass transfer driving force at high nitrate inlet amount, therefore, adsorption capacity increased, and more nitrate ions competed to the binding sites of AC leading to lower mass transfer rate [139]. By changing the flow rate (10–40 mL/min), the K_{Th} decreased (0.0026–0.0021 mL/mg.min). Thus, smaller initial amount and smaller flow rate enhanced nitrate fixed bed adsorption. The K_{YN} demonstrates the breakthrough curve shape. By enlarging the initial amount and flow rate, τ decreased, as a result of rapid saturation [136,137].

Similar observations were reported for the continuous nitrate adsorption on the $ZnCl_2$ modified coconut granular AC (CGAC) [73]. At adsorbent amounts of 10 g, 20 g, and 30 g, the breakthrough times were 200 min, 320 min, and 650 min, respectively. The highest uptakes of $ZnCl_2$-modied CGAC (10 g, 20 g, and 30 g) were 0.25 mg/g, 0.20 mg/g, and 0.17 mg/g, respectively. The breakthrough time enlarged with the use of more adsorbent which could be due to the large contacting time. The high NO_3^- capacity at the large bed height might due to enhanced surface area of adsorbent, which offered more adsorption sites for the continuous process [140]. In general, a rapid breakthrough curve was reported at larger flow rate at 20 mL/min. With increasing flow rate, the uptakes were 0.18 mg/g, 0.20 mg/g, and 0.27 mg/g, respectively. The breakthrough curve tended to be sharper as the flow rate enhanced. This could be related to the fact that NO_3^- had no sufficient time to attach with adsorbent at the large flow rate [141]. Rapid saturation and lower breakthrough time were reported for the adsorption with enlarging inlet NO_3^- amount. The nitrate uptakes of $ZnCl_2$-modied CGAC were 0.12 mg/g, 0.20 mg/g, and 0.26 mg/g, respectively. The highest uptake at 50 mg/L was more than those at 10 mg/L and 20 mg/L. This could be due to large inlet NO_3^- amount which enhanced the driving force for the adsorption process [142]. Thomas and Yoon–Nelson equations exhibited best fitting ($R^2 > 0.834$) to all the breakthrough data. Thus, these equations could describe the continuous nitrate adsorption which suggested that the film and pore diffusions were not the controlling steps [138].

In continuous adsorption, the breakthrough curves are significantly related to the flow rate, adsorbent amount, and inlet NO_3^- amount. Both Yoon–Nelson and Thomas equations exhibit well analysis for the experimental breakthrough data and in turn can be successfully applied for correlation of breakthrough curves.

9. Competitive adsorption

Aquatic systems usually contain several contaminants in the form of blends. This can affect their single uptake on an adsorbent because of the influence of competition and can also raise their single risk owing to the augmented effect. Thus, investigating the behavior of coadsorption and the nature of competition for these blends is important [92]. The removal performance of each pollutant in the blend can be represented by the uptakes ratio (R_q) in terms of Eq. (1) as follows:

$$R_q = q_{mi}/q_{si} \quad (1)$$

where q_{mi} (mg/g) is the uptake of adsorbate i in blended state, and q_{si} (mg/g) is the uptake of adsorbate *i* in single state. The type of competition is recognized as synergistic, antagonistic, and non-interactive at $R_q > 1$, $R_q < 1$, and $R_q = 1$, respectively. Various studies have included the coadsorption of nitrate with different inorganic anions and also with pollutants from other types on AC-based adsorbents [52].

The effect of most common co-existing (competing) inorganic anions such as, sulfate, chloride, phosphate, and carbonate on uptake of nitrate was identified in many studies. For instance, Mazarji et al. [63] tested the influence of these anions on the adsorption of NO_3^- by NaOH-cationic surfactant modified coconut shell-AC in a binary system consisting of different amount of anions (20, 40, 80 and 160 mg/L) and a constant nitrate amount of 40 mg/L. The other variables were fixed at the best values (e.g. 4 g/L adsorbent dose, 25 °C, pH 7, and 120 min). An antagonistic behavior was reported for the effect of anions on NO_3^- and the largest decline in nitrate uptake was observed for sulfate, followed by chloride, phosphate, and carbonate. The competition extent was inconsiderable for phosphate and carbonate due to the production of other materials (e.g. H_2CO_3 and $H_2PO_4^-$) which showed weak competition with nitrate for the active sites of AC in the neutral pH. Similar observations were reported by Cho et al. [88] for the nitrate adsorption on cationic polymer-treated granular activated carbon (AC from lignite) in the existence of chloride, sulfate, phosphate and carbonate. The highest competitive effect was obtained by sulfate, followed by chloride and phosphate with no influence by carbonate. The nitrate removal was declined by 35 %, 25 %, and 12 % in the existence of 5 mM sulfate, chloride and phosphate, respectively. The influence of inhibition was more considerable for anions with higher capability for ion exchange (i.e. chloride and sulfate) with quaternary ammonium groups on AC [143]. Phosphate tended to compete with nitrate for active sites via making inner-sphere complexes with the active groups of adsorbent.

Sulfate also had strong antagonistic effect on nitrate removal compared to other anions for the adsorption system of sulfate and chloride on HNO_3 modified commercial AC [62], and the adsorption system of sulfate, chloride, and bicarbonate by amine crosslinked magnetic banana bract AC [82], Muskmelon peel/H_2SO_4 AC- zinc ferrite $ZnFe_2O_4$ composite [97], the papaya seeds/H_2SO_4 AC- $CoFe_2O_4$ composite [105], Zr^{4+} ions modified chitosan-soya bean husk AC composite [100], Zn–Al LDHs/banana bract/H_2SO_4 AC composite [127].

Thus, negatively charged anions tend to compete with nitrate for adsorption sites of AC and the competition extent relates to different parameters like charge, size, electro negativity, and polarizability of the adsorbates etc. [113]. Sulphate can significantly affect nitrate removal owing to its larger anionic activity and charge which make it more easily fill the active sites of adsorbent. On the other hand, chloride has large electron affinity, which offers the considerable competition with nitrate [95].

Other co-adsorbates such as antibiotics and heavy metals were also included in the literature. Manjunath & Kumar [52] evaluated mono- and multi- adsorption of nitrate, phosphate, and metronidazole on *Prosopis juliflora*/H_2SO_4 derived activated carbon. The Langmuir and modified Langmuir equations were well used for the correlation of single and multi-component isotherm data. The highest uptake q_m of NO_3^- was 10.99 mg/g in the mono system and declined to 5.17 mg/g in the

multi-component system. Thus, the value of q_m was decreased by ~2 times and the ratio of $q_{m,multi}/q_{m,mono}$ was less than one (0.47), confirming that the NO_3^- removal was inhibited by the existence of other adsorbates. This antagonistic behavior could be related to the fact that the adsorbates competed for the specific number of vacant active sites on the adsorbent surface [53,135,144]. Moreover, in multi-adsorption, the change in composition of MNZ:P:N mixture from 0.1:0.25:0.5–10:25:50 exhibited a decline in the NO_3^- removal (88–19 %), which might be due the existence of more adsorption sites for a specific amount of adsorbent.

Tan et al. [65] showed a comparative study of nitrate, tetracycline, and arsenic(V) adsorption onto $FeCl_3$ modified (magnetic) AC (AF) derived from corn straw (*Zea mays L.*) by H_3PO_4 activation. The isotherms of NO_3^-, TC, and As(V) in the multi- systems were turned down-ward relative to their isotherms in the mono- systems, suggesting the existence of competition between adsorbates. At 50 mg/L TC, the NO_3^- uptakes reduced by 7.81 % and 10.19 % for AC and AF, respectively, relative to the mono-system. In a multi- system, the adsorption of TC molecules with large size might prevent the access of NO_3^- to the adsorbent sites, thus inhibit the uptake of NO_3^-. Besides, the adsorption of TC molecules on carbon-based adsorbents could exhibit a significant pore filling effect [145], thus decreasing the NO_3^- removal. The NO_3^- uptakes were declined by 35.94 % and 27.67 % in the existence of 30 mg/L As(V) for AC and AF, respectively. Moreover, NO_3^- showed lower effect on the As(V) uptake, particularly for AF. This might be related to the fact that As(V) strongly attracted with Fe-modified adsorbent relative to NO_3^- [146]. Similarly, TC strongly inhibited NO_3^- uptake compared to As(V) uptake. The values of q_m for NO_3^- adsorption on AC and AF were 1.28 and 2.06 mg/g (single system). The value of q_m for NO_3^- adsorption on AC and AF were 0.82 and 1.49 mg/g (binary system with 30 mg/L As(V)). The values of q_m for NO_3^- adsorption on AC and AF were 1.18 and 1.85 mg/g (binary system with 50 mg/L TC).

The presence of competitive adsorbates not only decreases the adsorption capacity but also can affect the equilibrium time of nitrate. For instance, Najmi et al. [56] explored the removal of nitrate, bicarbonate and sulfate by the *Glycyrrhiza glabra* residue/$ZnCl_2$ derived AC. The Langmuir equation offered well fitting for the nitrate adsorption in the absence and existence of competitor ions with the correlation coefficient R^2 >0.98. According to the Langmuir model, the maximum uptake for nitrate had reduced by 73.65 %, in the existence of competitor anions at 298 K. Moreover, the equilibrium state for nitrate adsorption was attained at 90 min, while for nitrate in the existence of anions 100 mg/L HCO^{-3} + 50 mg/L SO_2^{-4} the state was prolonged to 150 min. As the complexity of the solution increased, not only the equilibrium took place slower but also the removal is not as significant as the simple solutions [121].

10. Adsorption mechanism

The identification of adsorption mechanism is necessary to provide information about the type of interaction between adsorbates and the adsorbent molecules. It is also related to the adsorption isotherms, capacity, kinetics along with thermodynamics [147]. The mechanism of adsorption is mainly related to the molecular content, charge, and nature of the adsorbent. Moreover, it also changes with pH and various mechanisms can be reported for the same adsorbate/adsorbent system. According to the literature, the mechanism of the nitrate adsorption onto AC-based adsorbents may change and includes electrostatic interactions, ion-exchange, Lewis base-acid interaction, surface complexation, and hydrogen bonding. The majority of studies indicate that the nitrate adsorption onto ACs is controlled by electrostatic interactions and ion-exchange. For instance, Li et al. [80] reported that the mechanism of nitrate adsorption on zirconium chloride octahydrate / cetyltrimethylammonium bromide modified vetiver grass/KOH-AC (ZR/CTAB/VGAC) was mainly represented by the electrostatic interaction and ion exchange. FTIR and EDX results confirmed that CTAB and ZR were efficiently loaded on ZR/CTAB/VGAC. During the treatment with CTAB, a cationic surfactant in terms of CTAB was attached to the AC surface. Consequently, the positive charge in the surface of AC was increased, which could enhance the nitrate anions uptake by electrostatic interaction [84]. $ZrOCl_2$•8 H_2O is the source of Cl^- in composite, therefore ion exchange was also reported as the Cl^- ions existed in composite offered an exchange with nitrate ions [148]. Similar mechanism was reported for the adsorption of nitrate on polyaniline AC composite [46] and magnetic Mg-Fe/LDHs waste sludge-based $ZnCl_2$ AC composite [96].

Surface complexation was also indicated together with electrostatic interaction and ion-exchange as a mechanism step for the nitrate adsorption on many AC-based adsorbents. In this regard, Karthikeyan et al. [82] studied the mechanism of nitrate adsorption onto amine crosslinked magnetic banana bract/H_2SO_4 activated carbon (ACM@BBAC). FTIR and EDX results showed that the nitrate adsorption on ACM@BBAC was identified via electrostatic attraction, ion-exchange along with surface complexation mechanism. ACM@BBAC surface exhibited a positive charge in terms of $-NH^{2+}Cl^-$ and thereby it's might be linked with nitrate ions via the mechanisms of electrostatic interaction and ion-exchange [149]. Thus, the nitrate ions of larger electronegative charge tended to exchange the − OH groups and Cl^- ions via ion-exchange mechanism. Moreover, the Fe^{3+} ions of positive charges tended to adsorb the nitrate ions via electrostatic interaction and surface complexation [150]. Similar mechanism was suggested for the nitrate adsorption on Zn\Al-LDHs AC composite [127], Zn\Fe-LDHs AC composite [95], $ZnFe_2O_4$ AC composite [97], and $CoFe_2O_4$ AC composite [105].

Hydrogen bonding was also considered as a mechanism step for nitrate adsorption on a number of AC-based adsorbents besides electrostatic interaction and ion exchange mechanisms. For instance, Banu et al. [100] examined the mechanism of nitrate adsorption onto Zr^{4+} ions modified chitosan-soya bean husk AC composite (H_2SO_4 activation). $ZrOCl_2$·8 H_2O linked with active groups of chitosan and also Zr^{4+} ions entered the pores of AC which developed the adsorbent sites. The possible mechanism for the nitrate removal was by electrostatic interaction due to strong Lewis base-acid interaction and ion exchange along with H- bonding of nitrate ions with side −OH groups existed chitosan structure. The composite surface also contained Zr^{4+}, NH_3^+, OH_2^+ with positive charges which attracted the nitrate ions [151]. The mechanism of ion exchange mechanism was also reported as the Cl^- ions existed in Zr-CS-SAC composite tended to exchange with nitrate ions. Kiomarsipour et al. [72] also recorded that the mechanism of nitrate adsorption on amino-functionalized AC (3-aminopropyl trimethoxysilane) was represented by the electrostatic forces and hydrogen bonds between nitrate ions and positive functional groups (ammonium moieties).

Wang et al. [60] implied that the mechanism of NO_3^- adsorption on Mg/Al-LDHs apple branch/CO_2 AC composite included numerous steps (Fig. 5) such as electrostatic interaction, ion-exchange, physical adsorption, pore diffusion, surface complexation, and metal-linked bridges.

11. Regeneration and reusability

Reusability of exhausted adsorbents after their sufficient regeneration is a cost-effective and eco-friendly option for practical adsorption applications [46]. This option will avoid the need for a new adsorbent and prevent the appearance of new solid pollutants [94]. For this purpose, different chemical, biological, and thermal techniques have been applied for regenerating of saturated adsorbents. The first method is simple, efficient, inexpensive, and capable to regain adsorbates. It depends on using a convenient agent or eluent to regenerate the adsorbents [92].

Alkalis and acids along with salt and mixed eluents were applied to desorb nitrate anions from AC-based adsorbents (Table 5). Among these agents, NaOH was the most efficient and most widely applied for this purpose. In this regard, Shao et al. [58] observed that the regeneration

efficiency of various eluents for Zr/CTAB modified AC loaded with nitrate anions followed the order: NaOH > Na_2CO_3 > NaCl. The NO_3^- removal could be approximately 90 % after 4 recycling times, which suggested that the Zr/CTAB modified AC regenerated by NaOH had a convenient extent of reutilization. The successful use of NaOH as an eluent might be due to its ability to form Na^+ salts with some adsorbates which could be easily removed from the AC surface. Moreover, the large pH value obtained after NaOH addition could change the polarity of AC surface groups and thereby reduced the binding forces between the AC and adsorbate. AC-based adsorbents regenerated by 0.1 M NaOH presented the largest reuse times with insignificant decline in removal performance (Table 5). For instance, Zn\Fe-LDHs orange peel AC composite loaded with NO_3^- showed a few decline in adsorption efficiency from 85.5 % to 83.5 % after 5 cycles [95]. Also, raw *Carissa carandas* stems/H_2SO_4 derived AC underwent only 3.1 % decline in its NO_3^- uptake within 6 cycles. The structure of AC did not damage and was strong enough to act as an adsorbent. Beyond 6 cycles, there was an observable change and decline in nitrate uptake (Table 5). This might be related to the damage of some adsorption sites which reduced the AC performance [113].

Kalantary et al. [85] used 0.1 M HCl for regeneration of nitrate saturated Fe_3O_4 treated AC. The removal performance of AC for nitrate using 0.1 M HCl was approximately 98.9 %. The regeneration was performed within 10 cycles. A little decline in the removal performance of Fe_3O_4 modified AC adsorbent was reported (from 96.1 % to 87.5 %). High nitrate uptake was also reported on the adsorbent which offered the capability to be reused 10 times with insignificant reduction in the removal performance of adsorbent [152].

Banu et al. [100] used 0.1 M NaCl solution for regenerating Zr^{4+} ions modified chitosan-soya bean husk/H_2SO_4 AC composite loaded with nitrate. The existence of Cl^- ions in NaCl eluent tended to replace the nitrate ions in the exhausted adsorbent within a contact time of 60 min using 0.1 g of composite. The regenerated Zr-CS-SAC composite was applied for a next cycle. The nitrate uptake of regenerated composite was reported to be approximately 20.7 mg/g even beyond 5 regeneration cycles. Moreover, 75 % removal performance was obtained, and thereby the composite could act as an effective material for nitrate adsorption.

A mixture of NaOH and HCl was applied for regeneration of polyaniline-activated carbon composite saturated with nitrate [46]. Large pH value had a considerable adverse influence on nitrate adsorption. Furthermore, some active sites on AC surface could take protons (H^+) efficiently from water [62]. Therefore, 0.1 M NaOH and HCl eluents could act as desorbing and activating agents. In comparison to the initial removal performance for nitrate (91.2 %), the regenerated composite adsorbent still exhibited large removal performance of 87.5 %. Accordingly, this composite with a convenient reusing ability could be a practical adsorbent for commercial applications.

Thus, the data (Table 5) confirm that NaOH was the most applied and effective agent for the regeneration of activated carbon-based adsorbents loaded with nitrate. In particular, the use of 0.1 M NaOH eluent exhibits insignificant decline in adsorption performance within high cycles. Moreover, 0.1 M HCl also represents a high efficient eluent with a little decrease in adsorption performance within high regeneration cycle; however, its application needs more investigation.

12. Conclusions and future perspectives

The production of AC-based adsorbents and their application for removal of nitrate were reviewed. From the collected data, the most extensively applied AC-based adsorbents were in the forms of raw, modified, and composite. Chemical activation was the most frequently used process for the production of raw AC adsorbent compared to physical and physicochemical activations. Moreover, $ZnCl_2$ was the most applied chemical activating agent for production of AC and NaOH exhibited the highest surface area AC. For physical activation, steam was more utilized to produce AC relative to CO_2. In addition, the modified and composite forms of AC adsorbents showed an enhanced capacity for nitrate compared to raw AC adsorbents. In general, this enhancement in performance involved the development of surface properties by introducing additional and specific functional groups to the structure of raw adsorbents along with improving of pore properties in some cases. Several elements, including acids, alkali, surfactants, magnetic, urea, amines, $ZnCl_2$, etc. were applied for the treatment of AC-based adsorbents to maximize the performance for nitrate removal. Among these, surfactants, magnetic materials, and urea/amines were the best and most widely utilized agents for this purpose. The blending of two or more treatment steps also offered well treatment performance by combining the advantages of single steps. Incorporation of some materials such as layered double hydroxide, Fe_2O_3 nanoparticles, zero valent iron, zeolite, and chitosan into AC structure is an efficient way to enhance the performance of AC by developing its functionality and pore properties. Activation temperature and amount of activating agent variables exhibited significant effect on pore properties and performance of raw AC compared to activation time. Moreover, the effect of both initial nitrate concentration and AC dosage were more significant on the removal efficiency of nitrate relative to temperature and solution pH. Isotherm data for the majority of studies on nitrate/AC-based adsorbent systems were well correlated by Langmuir equation followed by the Freundlich model. Both Langmuir and Freundlich models also presented convenient correlations in some cases. The parameters of these isotherms confirmed the preferable nature of the nitrate adsorption. The pseudo-second order equation presented well analysis for the kinetic data and in some cases pseudo-first order was also applicable. The majority of studies reported negative magnitudes of ΔG° and positive magnitudes for both ΔS° and ΔH° of nitrate removal by AC-based adsorbents. Thomas and Yoon–Nelson equations were convenient for the design of continuous adsorption unit. An antagonistic behavior was mostly reported for the effect of competing adsorbates on NO_3^- and the decline in nitrate uptake in a mixture of anions followed the order: sulfate > chloride > phosphate > carbonate. The adsorption mechanism of nitrate/AC-based adsorbent systems mainly involved electrostatic attraction and ion exchange with the existence of other steps such as surface complexation, hydrogen bonding, physical adsorption, metal-bonded bridges, and pore diffusion. NaOH eluent was the most efficient and most widely applied for regenerating exhausted adsorbents.

AC-based materials are considered as effective adsorbents for nitrate due to their favorable pore characteristics, surface active groups enriched structures, and high removal performances. Accordingly, these materials were included in numerous studies. However, other items still want to be taken into account including (1) focusing on another form of AC such as AC fibers or cloths, (2) using other modifying agents and composite materials such as clay and biomass to further enhance the performance of raw AC adsorbents, (3) adopting co-pyrolysis and microwave techniques in production of AC-based adsorbents, (4) studying the influence of treatment factors like time, temperature, treating agent amount on characteristics of AC, (5) testing the impact of stirring speed and size of adsorbent particles on adsorption performance, (6) considering the ability of AC-based adsorbents to treat real polluted systems, (7) optimizing the regeneration performance and nitrate recovery from eluents, and (8) providing information about the economic feasibility and environmental effect of the prepared adsorbents to identify their convenient for large scale applications.

Declaration of Competing Interest

The authors declare that they have no known competing financial interests or personal relationships that could have appeared to influence the work reported in this paper.

Data availability

No data was used for the research described in the article.

Appendix A. Supporting information

Supplementary data associated with this article can be found in the online version at doi:10.1016/j.jaap.2022.105856.

References

[1] S. Dey, N. Haripavan, S.R. Basha, G.V. Babu, Removal of ammonia and nitrates from contaminated water by using solid waste bio-adsorbents, Curr. Res. Chem. Biol. 1 (2021), 100005.
[2] S. Tyagi, D. Rawtani, N. Khatri, M. Tharmavaram, Strategies for nitrate removal from aqueous environment using nanotechnology: a review, J. Water Process Eng. 21 (2018) 84–95.
[3] P. Loganathan, S. Vigneswaran, J. Kandasamy, Enhanced removal of nitrate from water using surface modification of adsorbents – a review, J. Environ. Manag. 131 (2013) 363–374.
[4] R.K.A. Amali, H.N. Lim, I. Ibrahim, N.M. Huang, Z. Zainal, S.A.A. Ahmad, Significance of nanomaterials in electrochemical sensors for nitrate detection: a review, Trends Environ. Anal. Chem. 31 (2021), e00135.
[5] B. Zhao, Z. Sun, Y. Liu, An overview of in-situ remediation for nitrate in groundwater, Sci. Total Environ. 804 (2022), 149981.
[6] S. Duan, T. Tong, S. Zheng, X. Zhang, S. Li, Achieving low-cost, highly selective nitrate removal with standard anion exchange resin by tuning recycled brine composition, Water Res. 173 (2020), 115571.
[7] R. Epsztein, O. Nir, O. Lahav, M. Green, Selective nitrate removal from groundwater using a hybrid nanofiltration–reverse osmosis filtration scheme, Chem. Eng. J. 279 (2015) 372–378.
[8] F.D. Belkada, O. Kitous, N. Drouiche, S. Aoudj, O. Bouchelaghem, N. Abdi, H. Grib, N. Mameri, Electrodialysis for fluoride and nitrate removal from synthesized photovoltaic industry wastewater, Sep. Purif. Technol. 204 (2018) 108–115.
[9] Y. Pang, J. Wang, Various electron donors for biological nitrate removal: a review, Sci. Total Environ. 794 (2021), 148699.
[10] I. Sanchis, E. Díaz, A.H. Pizarro, J.J. Rodríguez, A.F. Mohedano, Effect of water composition on catalytic reduction of nitrate, Sep. Purif. Technol. 255 (2021), 117766.
[11] A. Bhatnagar, M. Sillanpää, A review of emerging adsorbents for nitrate removal from water, Chem. Eng. J. 168 (2011) 493–504.
[12] Y. Liu, X. Zhang, J. Wang, A critical review of various adsorbents for selective removal of nitrate from water: structure, performance and mechanism, Chemosphere 291 (2022), 132728.
[13] T. Ye, K. Wang, C. Shuang, G. Zhang, A. Li, Reuse of spent resin for aqueous nitrate removal through bioregeneration, J. Clean. Prod. 224 (2019) 566–572.
[14] J.-K. Kang, S.-B. Kim, Synthesis of quaternized mesoporous silica SBA-15 with different alkyl chain lengths for selective nitrate removal from aqueous solutions, Microporous Mesoporous Mater. 295 (2020), 109967.
[15] J. Yang, H. Li, D. Zhang, M. Wu, B. Pan, Limited role of biochars in nitrogen fixation through nitrate adsorption, Sci. Total Environ. 592 (2017) 758–765.
[16] P. Ganesan, R. Kamaraj, S. Vasudevan, Application of isotherm, kinetic and thermodynamic models for the adsorption of nitrate ions on graphene from aqueous solution, J. Taiwan Inst. Chem. Eng. 44 (2013) 808–814.
[17] A. Adauto, M.R. Sun-Kou, Comparative study of anion removal using adsorbents prepared from a homoionic clay, Environmental, Nanotechnol. Monit. Manag. 15 (2021), 100476.
[18] V. Alimohammadi, M. Sedighi, E. Jabbari, Response surface modeling and optimization of nitrate removal from aqueous solutions using magnetic multi-walled carbon nanotubes, J. Environ. Chem. Eng. 4 (2016) 4525–4535.
[19] S. Jain, A. Bansiwal, R.B. Biniwale, S. Milmille, S. Das, S. Tiwari, P.S. Antony, Enhancing adsorption of nitrate using metal impregnated alumina, J. Environ. Chem. Eng. 3 (2015) 2342–2349.
[20] R. Gouran-Orimi, B. Mirzayi, A. Nematollahzadeh, A. Tardast, Competitive adsorption of nitrate in fixed-bed column packed with bio-inspired polydopamine coated zeolite, J. Environ. Chem. Eng. 6 (2018) 2232–2240.
[21] M. Abdelwaheb, K. Jebali, H. Dhaouadi, S. Dridi-Dhaouadi, Adsorption of nitrate, phosphate, nickel and lead on soils: risk of groundwater contamination, Ecotoxicol. Environ. Saf. 179 (2019) 182–187.
[22] Z. Lei, G. Cagnetta, X. Li, J. Qu, Z. Li, Q. Zhang, J. Huang, Enhanced adsorption of potassium nitrate with potassium cation on H_3PO_4 modified kaolinite and nitrate anion into Mg-Al layered double hydroxide, Appl. Clay Sci. 154 (2018) 10–16.
[23] A.M. Omer, R. Dey, A.S. Eltaweil, E.M. Abd El-Monaem, Z.M. Ziora, Insights into recent advances of chitosan-based adsorbents for sustainable removal of heavy metals and anions, Arab. J. Chem. 15 (2022), 103543.
[24] S. Dey, S.R. Basha, G.V. Babu, T. Nagendra, Characteristic and biosorption capacities of orange peels biosorbents for removal of ammonia and nitrate from contaminated water, Clean Mater. 1 (2021), 100001.
[25] M. Islam, P.C. Mishra, R. Patel, Physicochemical characterization of hydroxyapatite and its application towards Removal of nitrate from water, J. Environ. Manag. 91 (2010) 1883–1891.
[26] P. Mehrabinia, E. Ghanbari-Adivi, Examining nitrate surface absorption method from polluted water using activated carbon of agricultural wastes, Model. Earth Syst. Environ. 8 (2022) 1553–1561.
[27] M. Zhang, G. Song, D.L. Gelardi, L. Huang, E. Khan, O. Mašek, S.J. Parikh, Y. S. Ok, Evaluating biochar and its modifications for the removal of ammonium, nitrate, and phosphate in water, Water Res. 186 (2020), 116303.
[28] T. Sizmurv, T. Fresno, G. Akgül, H. Frost, E. Moreno-Jiménez, Biochar modification to enhance sorption of inorganics from water, Bioresour. Technol. 246 (2017) 34–47.
[29] M. Keshvardoostchokami, M. Majidi, A. Zamani, B. Liu, A review on the use of chitosan and chitosan derivatives as the bio-adsorbents for the water treatment: removal of nitrogen-containing pollutants, Carbohydr. Polym. 273 (2021), 118625.
[30] A.S. Eltaweil, A.M. Omer, H.G. El-Aqapa, N.M. Gaber, N.F. Attia, G.M. El-Subruiti, M.S. Mohy-Eldin, E.M. Abd El-Monaem, Chitosan based adsorbents for the removal of phosphate and nitrate: a critical review, Carbohydr. Polym. 274 (2021), 118671.
[31] C.V. Lazaratou, D.V. Vayenas, D. Papoulis, The role of clays, clay minerals and clay-based materials for nitrate removal from water systems: a review, Appl. Clay Sci. 185 (2020), 105377.
[32] N. Bellahsen, S. Kertész, Z. Pásztory, C. Hodúr, Adsorption of nutrients using low-cost adsorbents from agricultural waste and by-products – review, Prog. Agric. Eng. Sci. 14 (2018) 1–30.
[33] B. Bishayee, R.P. Chatterjee, B. Ruj, S. Chakrabortty, J. Nayak, Strategic management of nitrate pollution from contaminated water using viable adsorbents: an economic assessment-based review with possible policy suggestions, J. Environ. Manag. 303 (2022), 114081.
[34] A. Gizaw, F. Zewge, A. Kumar, A. Mekonnend, M. Tesfayee, A comprehensive review on nitrate and phosphate removal and recovery from aqueous solutions by adsorption, AQUA — water Infrastructure, Ecosyst. Soc. 70 (7) (2021) 921–947.
[35] M. Mohsenipour, S. Shahid, K. Ebrahimi, Removal techniques of nitrate from water, Asian J. Chem. 26 (23) (2014) 7881–7886.
[36] P. González-García, Activated carbon from lignocellulosics precursors: a review of the synthesis methods, characterization techniques and applications, Renew. Sustain. Energy Rev. 82 (2018) 1393–1414.
[37] M.J. Ahmed, Adsorption of quinolone, tetracycline, and penicillin antibiotics from aqueous solution using activated carbons: review, Environ. Toxicol. Pharmacol. 50 (2017) 1–10.
[38] E. Kacan, Optimum BET surface areas for activated carbon produced from textile sewage sludges and its application as dye removal, J. Environ. Manag. 166 (2016) 116–123.
[39] K.T. Wong, Y. Yoon, S.A. Snyder, M. Jang, Phenyl-functionalized magnetic palm-based powdered activated carbon for the effective removal of selected pharmaceutical and endocrine-disruptive compounds, Chemosphere 152 (2016) 71–80.
[40] L. Temdrara, A. Addoun, A. Khelifi, Development of olives tones-activated carbons by physical, chemical and physicochemical methods for phenol removal: a comparative study, Desalin. Water Treat. 53 (2015) 452–461.
[41] M.J. Ahmed, Preparation of activated carbons from date (Phoenix dactylifera L.) palm stones and application for wastewater treatments: review, Process Saf. Environ. Prot. 102 (2016) 168–182.
[42] M.J. Ahmed, Application of raw and activated Phragmites australis as potential adsorbents for wastewater treatments, Ecol. Eng. 102 (2017) 262–269.
[43] E. Menya, P.W. Olupot, H. Storz, M. Lubwama, Y. Kiros, Production and performance of activated carbon from rice husks for removal of natural organic matter from water: a review, Chem. Eng. Res. Des. 129 (2018) 271–296.
[44] Y. Gao, Q. Yue, B. Gao, A. Li, Insight into activated carbon from different kinds of chemical activating agents: a review, Sci. Total Environ. 746 (2020), 141094.
[45] S. Kilpimaa, H. Runtti, T. Kangas, U. Lassi, T. Kuokkanen, Physical activation of carbon residue from biomass gasification: novel sorbent for the removal of phosphates and nitrates from aqueous solution, J. Ind. Eng. Chem. 21 (2015) 1354–1364.
[46] Q. Hu, H. Liu, Z. Zhang, Y. Xie, Nitrate removal from aqueous solution using polyaniline modified activated carbon: Optimization and characterization, J. Mol. Liq. 309 (2020), 113057.
[47] S. Román, B. Ledesma, M.E. Fernandez, G.V. Nunell, P.R. Bonelli, A.L. Cukierman, Activated carbons developed in different activation conditions to improve nitrate adsorption performance, Bol. Grupo Esp. Carbón 42 (2016) 16–21.
[48] K. Daouda, A.N. Rahman, H.G. Valery, N.J. Nsami, A. Wahabou, K.J. Mbadcam, Adsorption equilibrium of nitrates ions onto oil palm shells based activated carbons, Glob. J. Sci. Front. Res. B Chem. 18 (B2) (2018) 37–52.
[49] Y. Zhang, X.-L. Song, S.-T. Huang, B.-Y. Geng, C.-H. Chang, I.-Y. Sung, Adsorption of nitrate ions onto activated carbon prepared from rice husk by NaOH activation, Desalin. Water Treat. 52 (2014) 4935–4941.
[50] C. Namasivayam, D. Sangeetha, Recycling of agricultural solid waste, coir pith: removal of anions, heavy metals, organics and dyes from water by adsorption onto $ZnCl_2$ activated coir pith carbon, J. Hazard. Mater. B135 (2006) 449–452.
[51] H. Demiral, G. Gündüzoğlu, Removal of nitrate from aqueous solutions by activated carbon prepared from sugar beet bagasse, Bioresour. Technol. 101 (2010) 1675–1680.
[52] S.V. Manjunath, M. Kumar, Evaluation of single-component and multi-component adsorption of metronidazole, phosphate and nitrate on activated carbon from Prosopıs julıflora, Chem. Eng. J. 346 (2018) 525–534.
[53] H.A. Hanafi, S.M. Abdel Azeema, Removal of nitrate and nitrite anions from wastewater using activated carbon derived from rice straw, J. Environ. Anal. Toxicol. 6 (2016) 346.

[54] W. Pan, R. Deng, Y. Cao, F. Xia, Q. Wu, L. Gu, Nitrate removal from aqueous solution by activated carbon prepared from shrimp shell, Desalin. Water Treat. 229 (2021) 134–144.
[55] S. Kilpimaa, H. Runtti, T. Kangas, U. Lassi, T. Kuokkanen, Removal of phosphate and nitrate over a modified carbon residue from biomass gasification, Chem. Eng. Res. Des. 92 (2014) 1923–1933.
[56] S. Najmi, M.S. Hatamipour, P. Sadeh, I. Najafipour, F. Mehranfar, Activated carbon produced from Glycyrrhiza glabra residue for the adsorption of nitrate and phosphate: batch and fixed-bed column studies, SN Appl. Sci. 2 (2020) 773.
[57] G.V. Nunell, M.E. Fernandez, P.R. Bonelli, A.L. Cukierman, Nitrate uptake from water by means of tailored adsorbents, Water Air Soil Pollut. 226 (2015) 278.
[58] Y. Shao, J. Li, X. Fang, Z. Yang, Y. Qu, M. Yang, W. Tan, G. Li, H. Wang, Chemical modification of bamboo activated carbon surface and its adsorption property of simultaneous removal of phosphate and nitrate, Chemosphere 287 (2022), 132118.
[59] A. Bhatnagar, M. Ji, Y.-H. Choi, W. Jung, S.-H. Lee, S.-J. Kim, G. Lee, H. Suk, H.-S. Kim, B. Min, S.-H. Kim, B.-H. Jeon, J.-W. Kang, Removal of nitrate from water by adsorption onto zinc chloride treated activated carbon, Sep. Sci. Technol. 43 (2008) 886–907.
[60] T. Wang, D. Zhang, K. Fang, W. Zhu, Q. Peng, Z. Xie, Enhanced nitrate removal by physical activation and Mg/Al layered double hydroxide modified biochar derived from wood waste: Adsorption characteristics and mechanisms, J. Environ. Chem. Eng. 9 (2021), 105184.
[61] M.M. Hamed, S.M. Yakout, H.S. Hassan, Solid phase extraction of nitrate and nitrite anions using naturally and available sorbent, J. Radioanal. Nucl. Chem. 295 (2013) 697–708.
[62] K. Ota, Y. Amano, M. Aikawa, M. Machida, Removal of nitrate ions from water by activated carbons (ACs)—Influence of surface chemistry of ACs and coexisting chloride and sulfate ions, Appl. Surf. Sci. 276 (2013) 838–842.
[63] M. Mazarji, B. Aminzadeh, M. Baghdadi, A. Bhatnagar, Removal of nitrate from aqueous solution using modified granular activated carbon, J. Mol. Liq. 233 (2017) 139–148.
[64] F. Xia, H. Yang, L. Li, Y. Ren, D. Shi, H. Chai, H. Ai, Q. He, L. Gu, Enhanced nitrate adsorption by using cetyltrimethylammonium chloride pre-loaded activated carbon, Environ. Technol. 41 (27) (2020) 3562–3572.
[65] G. Tan, Y. Mao, H. Wang, N. Xu, A comparative study of arsenic(V), tetracycline and nitrate ions adsorption onto magnetic biochars and activated carbon, Chem. Eng. Res. Des. 159 (2020) 582–591.
[66] M. Arbabi, S. Hemati, Z. Shamsizadeh, A. Arbabi, Nitrate removal from aqueous solution by almond shells activated with magnetic nanoparticles, Desalin. Water Treat. 80 (2017) 344–351.
[67] B. Kamarehie, E. Aghaali, S.A. Musavi, S.Y. Hashemi, A. Jafari, Nitrate removal from aqueous solutions using granular activated carbon modified with iron nanoparticles, Int. J. Eng. Trans. A Basics 31 (4) (2018) 554–563.
[68] G.V. Nunell, M.E. Fernandez, P.R. Bonelli, A.L. Cukierman, Nitrate uptake improvement by modified activated carbons developed from two species of pine cones, J. Colloid Interface Sci. 440 (2015) 102–108.
[69] A.R. Satayeva, C.A. Howell, A.V. Korobeinyk, J. Jandosov, V.J. Inglezakis, Z. A. Mansurov, S.V. Mikhalovsky, Investigation of rice husk derived activated carbon for removal of nitrate contamination from water, Sci. Total Environ. 630 (2018) 1237–1245.
[70] G.V. Nunell, M.E. Fernández, P.R. Bonelli, A.L. Cukierman, Conversion of biomass from an invasive species into activated carbons for removal of nitrate from wastewater, Biomass Bioenergy 44 (2012) 87–95.
[71] R.B.N. Lekene, D. Kouotou, N.O. Ankoro, A.P.-M.S. Kouoh, J.N. Ndi, J.M. Ketcha, Development and tailoring of amino-functionalized activated carbon based Cucumerupsi manni Naudin seed shells for the removal of nitrate ions from aqueous solution, J. Saudi Chem. Soc. 25 (2021), 101316.
[72] N. Kiomarsipour, M. Alizadeh, M. Alizadeh, K. Ghani, Synthesis and surface-functionalizing of ordered mesoporous carbon CMK-3 for removal of nitrate from aqueous solution as an effective adsorbent, Diam. Relat. Mater. 116 (2021), 108419.
[73] L. Liu, M. Ji, F. Wang, Adsorption of nitrate onto $ZnCl_2$-modified coconut granular activated carbon: kinetics, characteristics, and adsorption dynamics, Adv. Mater. Sci. Eng. 2018 (2018), 1939032.
[74] M.A. Khan, Y.-T. Ahn, M. Kumar, W. Lee, B. Min, G. Kim, D.-W. Cho, W.B. Park, B.-H. Jeon, Adsorption studies for the removal of nitrate using modified lignite granular activated carbon, Sep. Sci. Technol. 46 (16) (2011) 2575–2584.
[75] C. Yuan, Y. Huang, F.S. Cannon, C. Geng, Z. Liang, Z. Zhao, Removing PFOA and nitrate by quaternary ammonium compounds modified carbon and its mechanisms analysis: Effect of base, acid or oxidant pretreatment, Chemosphere 242 (2020), 125233.
[76] K. Kino, T. Sakamoto, J. Yuan, Y. Amano, M. Machida, Quaternary nitrogen functionalized carbonaceous adsorbents to remove nitrate from aqueous phase, Catal. Today 388– 389 (2022) 269–273.
[77] S.M. Yakout, A.A. Mostafa, Adsorption kinetics of nitrate by activated carbon from wastewater, J. Anim. Vet. Adv. 12 (17) (2013) 1399–1403.
[78] A. Rezaee, H. Godini, S. Dehestani, A. Khavanin, Application of impregnated almond shell activated carbon by zinc and zinc sulfate for nitrate removal from water, Iran. J. Environ. Health Sci. Eng. 5 (2) (2008) 125–130.
[79] M. Machida, T. Goto, Y. Amano, T. Iida, Adsorptive removal of nitrate from aqueous solution using nitrogen doped activated carbon, Chem. Pharm. Bull. 64 (11) (2016) 1555–1559.
[80] J. Li, X. Fang, M. Yang, W. Tan, H. Zhang, Y. Zhang, G. Li, H. Wang, The adsorption properties of functionalization vetiver grass-based activated carbon: the simultaneous adsorption of phosphate and nitrate, Environ. Sci. Pollut. Res. 28 (2021) 40544–40554.
[81] M. Ahmadi, H. Rahmani, B. Ramavandi, B. Kakavandi, Removal of nitrate from aqueous solution using activated carbon modified with Fenton reagents, Desalin. Water Treat. 76 (2017) 265–275.
[82] P. Karthikeyan, S. Vigneshwaran, S. Meenakshi, Removal of phosphate and nitrate ions from water by amine crosslinked magnetic banana bract activated carbon and its physicochemical performance, Environ. Nanotechnol., Monit. Manag. 13 (2020), 100294.
[83] A. Bhatnagar, W. Hogland, M. Marques, M. Sillanpää, An overview of the modification methods of activated carbon for its water treatment applications, Chem. Eng. J. 219 (2013) 499–511.
[84] O. Allalou, D. Miroud, M. Belmedani, Z. Sadaoui, Performance of surfactant-modified activated carbon prepared from dates wastes for nitrate removal from aqueous solutions, Environ. Prog. Sustain. Energy 38 (s1) (2018) S403–S411.
[85] R.R. Kalantary, E. Dehghanifard, A. Mohseni-Bandpi, L. Rezaei, A. Esrafili, B. Kakavandi, A. Azari, Nitrate adsorption by synthetic activated carbon magnetic nanoparticles: kinetics, isotherms and thermodynamic studies, Desalin. Water Treat. 57 (35) (2016) 16445–16455.
[86] M. Zhang, B. Gao, S. Varnoosfaderani, A. Hebard, Y. Yao, M. Inyang, Preparation and characterization of a novel magneticbiochar for arsenic removal, Bioresour. Technol. 130 (2013) 457–462.
[87] E.I. El-Shafey, S.N.F. Ali, S. Al-Busafi, H.A.J. Al-Lawati, Preparation and characterization of surface functionalized activated carbons from date palm leaflets and application for methylene blue removal, J. Environ. Chem. Eng. 4 (2016) 2713–2724.
[88] D.-W. Cho, C.-M. Chon, Y. Kim, B.-H. Jeon, F.W. Schwartz, E.-S. Lee, H. Song, Adsorption of nitrate and Cr(VI) by cationic polymer-modified granular activated carbon, Chem. Eng. J. 175 (2011) 298–305.
[89] A. Gierak, I. Łazarska, Adsorption of nitrate, nitrite, and ammonium ions on carbon adsorbents, Adsorpt. Sci. Technol. 35 (7–8) (2017) 721–727.
[90] O. Zanella, I.C. Tessaro, L.A. Féris, Study of $CaCl_2$ as an agent that modifies the surface of activated carbon used in sorption/treatment cycles for nitrate removal, Braz. J. Chem. Eng. 31 (1) (2014) 205–210.
[91] O. Zanella, I.C. Tessaro, L.A. Féris, Nitrate sorption on activated carbon modified with $CaCl_2$: equilibrium, isotherms and kinetics, Chem. Ind. Chem. Eng. Q 21 (1) (2015) 23–33.
[92] M.J. Ahmed, B.H. Hameed, E.H. Hummadi, Insight into the chemically modified crop straw adsorbents for the enhanced removal of water contaminants: a review, J. Mol. Liq. 330 (2021), 115616.
[93] N. Tahir, H.N. Bhatti, M. Iqbal, S. Noreen, Biopolymers composites with peanut hull waste biomass and application for crystal violet adsorption, Int. J. Biol. Macromol. 94 (2017) 210–220.
[94] M.J. Ahmed, B.H. Hameed, E.H. Hummadi, Review on recent progress in chitosan/chitin-carbonaceous material composites for the adsorption of water pollutants, Carbohydr. Polym. 247 (2020), 116690.
[95] P. Karthikeyan, S. Meenakshi, Enhanced removal of phosphate and nitrate ions by a novel Zn-Fe LDHs-activated carbon composite, Sustain. Mater. Technol. 25 (2020), e00154.
[96] O. Alagha, M.S. Manzar, M. Zubair, I. Anil, N.D. Mu'azu, A. Qureshi, Magnetic Mg-Fe/LDH intercalated activated carbon composites for nitrate and phosphate removal from wastewater: insight into behavior and mechanisms, Nanomaterials 10 (2020) 1361.
[97] P. Karthikeyan, P. Sirajudheen, M.R. Nikitha, S. Meenakshi, Removal of phosphate and nitrate via a zinc ferrite@activated carbon hybrid composite under batch experiments: Study of isotherm and kinetic equilibriums, Environ. Nanotechnol., Monit. Manag. 14 (2020), 100378.
[98] N. Mehrabi, M. Soleimani, M.M. Yeganeha, H. Sharififard, Parameters optimization for nitrate removal from water using activated carbon and composite of activated carbon and Fe_2O_3 nanoparticles, RSC Adv. 5 (2015) 51470–51482.
[99] J.S. Hong, J.K. Suh, Study on simultaneous removal of nitrogen and phosphorus using zeocarbon, Carbon Lett. 11 (2) (2010) 112–116.
[100] H.T. Banu, P. Karthikeyan, S. Meenakshi, Zr^{4+} ions embedded chitosan-soya bean husk activated bio-char composite beads for the recovery of nitrate and phosphate ions from aqueous solution, Int. J. Biol. Macromol. 130 (2019) 573–583.
[101] S. Sepehri, M.M. Nakhjavanimoghaddam, Batch removal of aqueous nitrate ions using an effective nano-biocomposite, Glob. NEST J. 21 (3) (2019) 265–275.
[102] D. Zhu, J. Zuo, Y. Jiang, J. Zhang, J. Zhang, C. Wei, Carbon-silica mesoporous composite in situ prepared from coal gasification fine slag by acid leaching method and its application in nitrate removing, Sci. Total Environ. 707 (2020), 136102.
[103] D. Huang, C. Liu, C. Zhang, R. Deng, R. Wang, W. Xue, H. Luo, G. Zeng, Q. Zhang, X. Guo, Cr(VI) removal from aqueous solution using biochar modified with Mg/Allayered double hydroxide intercalated with ethylenediaminetetraacetic acid, Bioresour. Technol. 276 (2019) 127–132.
[104] Q. Zheng, L. Yang, D. Song, S. Zhang, H. Wu, S. Li, X. Wang, High adsorption capacity of Mg–Al-modified biochar for phosphate and its potential for phosphate interception in soil, Chemosphere 259 (2020), 127469.
[105] P. Karthikeyan, S. Vigneshwaran, J. Preethi, S. Meenakshi, Preparation of novel cobalt ferrite coated-porous carbon composite by simple chemical co-precipitation method and their mechanistic performance, Diam. Relat. Mater. 108 (2020), 107922.
[106] N.A. Rashidi, S. Yusup, A review on recent technological advancement in the activated carbon production from oil palm wastes, Chem. Eng. J. 314 (2017) 277–290.

[107] R.H. Hesas, W.M.A. Wan Daud, J.N. Sahu, A. Arami-Niya, The effects of a microwave heating method on the production of activated carbon from agricultural waste: a review, J. Anal. Appl. Pyrolysis 100 (2013) 1–11.
[108] P. Mehrabinia, E. Ghanbari-Adivi, R. Fattahi, H.A. Samimi, J. Kermannezhad, Nitrate removal from agricultural effluent using sugarcane bagasse active nanosorbent, J. Appl. Water Eng. Res. 10 (3) (2022) 238–249.
[109] D. Kalderis, D. Koutoulakis, P. Paraskeva, E. Diamadopoulos, E. Otal, J.O.D. Valle, C. Fernańdez-Pereira, Adsorption of polluting substances on activated carbons prepared from rice husk and sugarcane bagasse, Chem. Eng. J. 144 (2008) 42–50.
[110] N.S. Awwad, H.M.H. Gad, M.I. Ahmad, H.F. Aly, Sorption of lanthanum and erbium from aqueous solution by activated carbon prepared from rice husk, Colloid Surf. B 81 (2010) 593–599.
[111] X. Song, Y. Zhang, C. Chang, Novel method for preparing activated carbons with high specific surface area from rice husk, Ind. Eng. Chem. Res. 51 (2012) 15075–15081.
[112] D. Angın, E. Altintig, T.E. Köse, Influence of process parameters on the surface and chemical properties of activated carbon obtained from biochar by chemical activation, Bioresour. Technol. 148 (2013) 542–549.
[113] W.K. Biftu, M. Suneetha, K. Ravindhranath, Sequential adsorptive removal of phosphate, nitrate and chromate from polluted water using active carbon derived from stems of Carissa carandas plant, Water Pract. Technol. 16 (1) (2021) 117–134.
[114] I. Rouabeh, M. Amrani, Equilibrium modeling for adsorption of NO_3 from aqueous solution on activated carbon produced from pomegranate peel, Adv. Environ. Res. 1 (2) (2012) 143–151.
[115] A. Khataee, A. Khaniy, 2009. Modeling of nitrate adsorption on granular activated carbon (GAC) using artificial neural network (ANN), Int. J. Chem. React. Eng. 7 (2009), A5.
[116] N. Taoufik, A. Elmchaouri, S.A. Korili, A. Gil, Optimizing the removal of nitrate by adsorption onto activated carbon using response surface methodology based on the central composite design, J. Appl. Water Eng. Res. 8 (1) (2020) 66–77.
[117] M.J. Ahmed, B.H. Hameed, Insights into the isotherm and kinetic models for the coadsorption of pharmaceuticals in the absence and presence of metal ions: A review, J. Environ. Manag. 252 (2019), 109617.
[118] H. Nassar, A. Zyoud, A. El-Hamouz, R. Tanbour, N. Halayqa, H.S. Hilal, Aqueous nitrate ion adsorption/desorption by olive solid waste-based carbon activated using $ZnCl_2$, Sustain. Chem. Pharm. 18 (2020), 100335.
[119] D. Schwantes, A.C.G. Jr, D.C. Schons, T.G. Veiga, R.C. Diel, V. Schwantes, Nitrate adsorption using sugar cane bagasse physicochemically changed, J. Agric. Environ. Sci. 4 (1) (2015) 51–59.
[120] M.K. Asl, A.H. Hasani, E. Naserkhaki, Evaluation of nitrate removal from water using activated carbon and clinoptilolite by adsorption method, Biosci. Biotechnol. Res. Asia 13 (2) (2016) 1045–1054.
[121] S. Jamaliniya, O.D. Basu, S. Suresh, E. Musvoto, A. Mackintosh, Kinetic analysis of sucrose activated carbon for nutrient removal in water, H_2 Open J. 3 (1) (2020) 208–220.
[122] R. Mahmudov, C.P. Huang, Selective adsorption of oxyanions on activated carbon exemplified by Filtrasorb 400 (F400), Sep. Purif. Technol. 77 (2011) 294–300.
[123] K. Ohe, Y. Nagae, S. Nakamura, Y. Baba, Removal of nitrate anion by carbonaceous materials prepared from bamboo and coconut shell, J. Chem. Eng. Jpn. 36 (4) (2003) 511–515.
[124] T. Iida, Y. Amano, M. Machida, F. Imazeki, Effect of surface property of activated carbon on adsorption of nitrate ion, Chem. Pharm. Bull. 61 (11) (2013) 1173–1177.
[125] S. Dehestaniathar, A. Rezaee, Adsorption of nitrate from aqueous solution using activated carbon-supported Fe0, $Fe_2(SO_4)_3$, and $FeSO_4$, J. Adv. Environ. Health Res 2 (3) (2014) 181–188.
[126] A. Azhdarpoor, L. Khosrozadeh, M. Shirdarreh, Nitrate removal from water using complex of activated carbon with Fe^{3+}, Water Supply 19 (4) (2019) 1097–1102.
[127] P. Karthikeyan, S. Meenakshi, Synthesis and characterization of Zn–Al LDHs/activated carbon composite and its adsorption properties for phosphate and nitrate ions in aqueous medium, J. Mol. Liq. 296 (2019), 111766.
[128] M.J. Ahmed, Adsorption of non-steroidal anti-inflammatory drugs from aqueous solution using activated carbons: review, J. Environ. Manag. 190 (2017) 274–282.
[129] M.J. Ahmed, Application of agricultural based activated carbons by microwave and conventional activations for basic dye adsorption: review, J. Environ. Chem. Eng. 4 (2016) 89–99.
[130] N. Öztürk, T.E. Bektaş, Nitrate removal from aqueous solution by adsorption onto various materials, J. Hazard. Mater. B112 (2004) 155–162.
[131] M.J. Ahmed, B.H. Hameed, Removal of emerging pharmaceutical contaminants by adsorption in a fixed bed column: a review, Ecotoxicol. Environ. Saf. 149 (2018) 257–266.
[132] J. Lemus, C. Moya, M.A. Gilarranz, J.J. Rodriguez, J. Palomar, Fixed-bed adsorption of ionic liquids onto activated carbon from aqueous phase, J. Environ. Chem. Eng. 5 (2017) 5347–5351.
[133] M.S. Hussein, M.J. Ahmed, Fixed bed and batch adsorption of benzene and toluene from aromatic hydrocarbons on 5A molecular sieve zeolite, Mater. Chem. Phys. 181 (2016) 512–517.
[134] A.U. Rajapaksha, R. Selvasembian, A. Ashiq, V. Gunarathne, A. Ekanayake, V. O. Perera, H. Wijesekera, S. Mia, M. Ahmad, M. Vithanage, Y.S. Oki, A systematic review on adsorptive removal of hexavalent chromium from aqueous solutions: recent advances, Sci. Total Environ. 809 (2022), 152055.
[135] S.V. Manjunath, M. Kumar, Simultaneous removal of antibiotic and nutrients via Prosopis juliflora activated carbon column: performance evaluation, effect of operational parameters and breakthrough modeling, Chemosphere 262 (2021), 127820.
[136] U. Kumari, A. Mishra, H. Siddiqi, B.C. Meikap, Effective defluoridation of industrial wastewater by using acid modified alumina in fixed-bed adsorption column: experimental and breakthrough curves analysis, J. Clean. Prod. 279 (2021), 123645.
[137] N. Rahman, M.F. Khan, Nitrate removal using poly-o-toluidine zirconium(IV) ethylenediamine as adsorbent: batch and fixed-bed column adsorption modeling, J. Water Process Eng. 9 (2016) 254–266.
[138] W.M. Golie, S. Upadhyayula, Continuous fixed-bed column study for the removal of nitrate fromwater using chitosan/alumina composite, J. Water Process Eng. 12 (2016) 58–65.
[139] A. Ansari, E.T. Nadres, M. D`o, D.F. Rodrigues, Investigation of the removal and recovery of nitrate by an amine-enriched composite under different fixed-bed column conditions, Process Saf. Environ. Prot. 150 (2021) 365–372.
[140] L. Yanyan, T.A. Kurniawan, M. Zhu, T. Ouyang, R. Avtar, M.H.D. Othman, B. T. Mohammad, A.B. Albadarin, Removal of acetaminophen from synthetic wastewater in a fixed-bed column adsorption using low-cost coconut shell waste pretreated with NaOH, HNO_3, ozone, and/or chitosan, J. Environ. Manag. 226 (2018) 365–376.
[141] A. Olgun, N. Atar, S. Wang, Batch and column studies of phosphate and nitrate adsorption on waste solids containing boron impurity, Chem. Eng. J. 222 (2013) 108–119.
[142] J. Pan, B. Gao, W. Song, X. Xu, B. Jin, Q. Yue, Column adsorption and regeneration study of magnetic biopolymer resin for perchlorate removal in presence of nitrate and phosphate, J. Clean. Prod. 213 (2019) 762–775.
[143] J. Patterson, R. Parette, F.S. Cannon, C. Lutes, T. Henderson, Competition of anions with perchlorate for exchange sites on cationic surfactant-tailored GAC, Environ. Eng. Sci. 28 (2011) 249–256.
[144] F. Ogata, D. Imai, N. Kawasaki, Adsorption of nitrate and nitrite ions onto carbonaceous material produced from soybean in a binary solution system, J. Environ. Chem. Eng. 3 (2015) 155–161.
[145] X. Zhu, Y. Liu, C. Zhou, G. Luo, S. Zhang, J. Chen, A novel porous carbon derived from hydrothermal carbon for efficient adsorption of tetracycline, Carbon 77 (2014) 627–636.
[146] R. He, Z. Peng, H. Lyu, H. Huang, Q. Nan, J. Tang, Synthesis and characterization of an iron-impregnated biochar for aqueous arsenic removal, Sci. Total Environ. 612 (2018) 1177–1186.
[147] I.W. Almanassra, V. Kochkodan, G. Mckay, M.A. Atieh, T. Al-Ansari, Review of phosphate removal from water by carbonaceous sorbents, J. Environ. Manag. 287 (2021), 112245.
[148] W. Xiong, J. Tong, Z. Yang, Adsorption of phosphate from aqueous solution using iron-zirconium modified activated carbon nanofiber: performance and mechanism, J. Colloid Interface Sci. 493 (2017) 17–23.
[149] H.T. Banu, S. Meenakshi, S, One pot synthesis of chitosan grafted quaternized resin for the removal of nitrate and phosphate from aqueous solution, Int. J. Biol. Macromol. 104 (2017) 1517–1527.
[150] I.A. Kumar, N. Viswanathan, N, Development and reuse of amine-grafted chitosan hybrid beads in the retention of nitrate and phosphate, J. Chem. Eng. Data 63 (2018) 147–158.
[151] J. Chen, L.-G. Yan, H.-Q. Yu, S. Li, L.-L. Qin, G.Q. Liu, Y.-F. Li, B. Du, Efficient removal of phosphate by facile prepared magnetic diatomite and illite clay from aqueous solution, Chem. Eng. J. 287 (2016) 162–172.
[152] H.Y. Zhu, Y.Q. Fu, R. Jiang, J.H. Jiang, L. Xiao, G.-M. Zeng, S.L. Zhao, Y. Wang, Adsorption removal of congo red onto magnetic cellulose/Fe_3O_4/activated carbon composite: equilibrium, kinetic and thermodynamic studies, Chem. Eng. J. 173 (2011) 494–502.